An ERF transcription factor PTI5, a novel regulator of endophyte community maintenance in potato

Tjaša Lukan[1*], Barbara Kraigher[2], Karmen Pogačar[1,3], Katja Stare[1], Teja Grubar Kovačič[1], Maja Zagorščak[1], Marko Petek[1], Polonca Stefanic[2], Anže Vozelj[1,3], Valentina Levak[1,3], Tjaša Mahkovec Povalej[1], Juan M. García[4], Maria J. Pozo[4], Ines Mandić-Mulec[2+], Kristina Gruden[1+*]

[1]Department of Biotechnology and Systems Biology, National Institute of Biology, Ljubljana, Slovenia

[2]Chair of Microbial Ecology and Physiology, Department of Microbiology, Biotechnical Faculty, University of Ljubljana, Ljubljana, Slovenia

[3]Jožef Stefan International Postgraduate School, Jamova cesta 39, 1000 Ljubljana, Slovenia

[4]Department of Soil and Plant Microbiology, Estación Experimental del Zaidín (CSIC), Granada, Spain

[+-]These authors share last authorship

*-corresponding authors

Kristina Gruden (kristina.gruden@nib.si)

ORCID IDs: Tjaša Lukan (0000-0002-6235-2816), Barbara Kraigher (0000-0002-3345-272X), Karmen Pogačar (0000-0001-5190-7217), Katja Stare (0000-0002-3999-9400), Teja Grubar Kovačič (), Maja Zagorščak (0000-0002-1669-6482), Marko Petek (0000-0003-3644-7827), Polonca Štefanič (0000-0002-9444-597X), Anže Vozelj (0009-0003-8758-3244), Valentina Levak (0000-0001-5975-4032), Tjaša Mahkovec Povalej (0000-0003-3706-2371), Juan M. García (0000-0002-4242-5440), Maria J. Pozo (0000-0003-2780-9793), Ines Mandic Mulec (0000-0002-7629-3255), Kristina Gruden (0000-0001-5906-8569)

Keywords: *Solanum tuberosum, Bacillus subtilis*, arbuscular mycorrhizal fungus *Rhizophagus irregularis*, ERF transcription factor PTI5, endophyte colonisation mechanism, microbial triggered immunity

ABSTRACT

We have recently identified ERF transcription factor PTI5 as a susceptibility factor, negatively regulating immune response to diverse pathogens. Here we investigated the processes involved in

colonisation of potato with beneficial organisms. RNAseq showed that at the time of *Bacillus subtilis* biofilm establishment, immune responses in interacting roots were attenuated, and complex transcriptional network was triggered, with ethylene signalling being a central module and PTI5 strongly induced. Interestingly, the response is intensified if plants are inoculated by two antagonistic *B. subtilis* strains. While PTI5 is not involved in the establishment of biofilm on roots, we show that bacterial abundance increases in PTI5-silenced plants. Remarkably, root colonization by the arbuscular mycorrhizal fungus *Rhizophagus irregularis* was also higher in the PTI5-silenced plants. PTI5 is thus involved both in blocking defence against harmful and blocking colonisation with beneficial microbes. Such mechanistic understanding of plant–microbe interaction paves the way for sustainable crop management.

INTRODUCTION

Plant-microbe and microbe–microbe interactions in the rhizosphere determine plant health and productivity.[1] Beneficial microorganisms are common in rhizosphere soils. Some can endophytically colonize plants, frequently improving plant nutrition and plant growth, and protect plants from disease and abiotic stresses through a wide variety of mechanisms.[2,3] They can be efficient and environmentally friendly alternatives to chemical pesticides and fertilizers, due to their multiple benefits for the plants and their long shelf life, which is comparable with that of agrochemicals.[4] However, the current limitation for a wider adoption of microbial inoculants in agriculture is reproducibility of the results under field conditions.[5] Additional knowledge, such as a deeper understanding of the mechanisms involved in plant colonization and maintenance of the plant microbiome is required to improve the use of microbes as plant protectants.[6]

The plant immune system is central in shaping the plant response to beneficial and pathogenic microorganisms, regulating the extension and successful colonization of plant tissues by mutualistic organisms and preventing the invasion of the parasitic ones. Recognition of pathogens leads to the

55 activation of interconnected plant hormonal signaling pathways mediating downstream
56 transcriptional reprogramming resulting in effective defense responses.[7,8] When plant interacts with
57 beneficial microbes, microbe triggered immunity (MTI) is activated similarly as in interaction with
58 pathogens.[9] Beneficial microbes developed several strategies to overcome this immune response and
59 colonize the plant. One option to avoid effective recognition is by modifying the microbe-associated-
60 pattern, recognized by immunity, for example flagellin. Alternatively, the microbes develop tolerance
61 to toxic compounds produced, e.g. reactive oxidative species (ROS) or they actively suppress MTI.[10]
62 They can also modify metabolism of plant to allow for easier penetration, for example suppress
63 synthesis of suberin.[11]

64 Successful colonization by beneficial microbes can induce resistance to pathogenic bacteria and
65 herbivores. Mechanisms of induced resistance (IR) are not well understood, but it has been shown to
66 involve jasmonic acid (JA), salicylic acid (SA) and ethylene signaling pathways.[11, 12, 13] Several
67 individual transcription factors have been shown also to be important for the establishment of the IR
68 state. As described for bacteria, root colonization by beneficial fungi can also boost plant immunity.
69 For example, root colonization by arbuscular mycorrhizal fungi is tightly regulated and the
70 modulation of immune responses during the symbiosis establishment can also leads to induced
71 resistance in systemic tissues.[15] Therefore, understanding the fine-tuned regulation of plant immune
72 responses during colonization by beneficials is essential for optimizing bioinoculant-based strategies
73 in agriculture, allowing their establishment and promoting their benefits in plant health.

74 In the case of bacteria, social behavior has been proven to be crucial for the success in colonizing
75 plant tissues. Bacteria often exist in multicellular groups of cells called biofilms,[16] where they engage
76 in competition for resources but also in cooperative (synergistic) interactions that enhance
77 community productivity.[17] These social engagements are most often mediated through secreted
78 molecules that are believed to have a profound impact on bacterial diversity, spatial organization,
79 and ecological functions.[16,18] *B. subtilis* species are capable of different forms of social interactions

80 besides biofilm formation, such as quorum sensing (QS), group motility (swarming), and kin
81 discrimination.[19] Non-kin *B. subtilis* strains form a striking boundary between approaching
82 swarms,[20,21] exclude a non-kin competitor from a common swarm,[22] and do not mix on *Arabidopsis*
83 *thaliana* roots, while kin strains merge on solid medium and cohabit root surfaces.[20] *B. subtilis* strains
84 also produce a range of antibiotics, surfactants, secondary metabolites, and bioactive volatiles
85 expected to modulate social interactions between bacteria and with the plant.[20,21,23,24]

86 *B. subtilis* QS system comprises the signalling peptide ComX, which positively regulates the synthesis
87 of surfactin (encoded by Srf operon), one of the most potent surfactants and a lipopeptide
88 antibiotic.[19,25] Surfactin acts as a signalling molecule during biofilm formation, promotor of horizontal
89 gene transfer and as an inducer of physiological changes in plants during colonization with
90 bacteria.[25,26,27,28,29] Despite evidence for *in situ* QS dependent expression of surfactin, the link
91 between QS and surfactin on plant roots and how QS affects plant colonisation and plant immune
92 response is less understood.

93 As potato, the third most important crop in the world, is exceptionally sensitive to a wide range of
94 environmental stresses,[31] studying its interaction with beneficial microbes is crucial to ensure an
95 efficient environmentally friendly system of plant protection based on modulation of its microbiome.
96 The aim of this study was to investigate mechanisms involved in the interaction between potato and
97 beneficial microbes. Different *B. subtilis* strains and mutants were used to investigate the principles
98 of bacterial social interactions and their interaction with the plant. We identified transcription factor
99 PTI5 as a potential regulatory hub for *B. subtilis* endophytic colonization and further investigated its
100 role in the plant–bacteria interaction using transgenic plants with silenced PTI5. We here show that
101 *B. subtilis* abundance is increased in systemic tissue of plants with silenced PTI5, suggesting that PTI5
102 maintains optimal *B. subtilis* abundance in colonized plants. Interestingly, a similar function was
103 confirmed also for the establishment of the mutualistic symbiosis between potato and arbuscular
104 mycorrhizal fungi.

105

106 **RESULTS**

107 **Stable *B. subtilis* biofilm formation on potato roots coincides with first transcriptional responses in**

108 **plant roots**

109 We here studied the response of potato to colonization by two different *B. subtilis* strains (PS-216

110 and PS-218). Both formed biofilm on potato roots (Figure S1). As our aim was to capture both initial

111 events in biofilm establishment as well as long-term effects of potato–*B. subtilis* interaction, we first

112 determined timing of biofilm establishment on potato roots and transcriptional responses in the

113 plant. We selected eight genes known to be involved in potato immune response as potential

114 indicators of potato MTI to *B. subtilis* colonization[32,33] and followed their expression in potato roots

115 and shoot tissue. The genes showed diverse expression profiles, which were for some genes tissue

116 specific (Figure S2, Table S1). Two genes, an ERF transcription factor PTI5, which requires an active

117 ethylene pathway for the activation and mediates crosstalk of ethylene and SA pathways[33] and a

118 gene involved in JA synthesis, 13LOX,[32] were reproducibly upregulated in roots and shoots 24 hours

119 post-bacterial inoculation (Figure 1, Figure S2, Table S1). The results were similar for both tested *B.*

120 *subtilis* strains (Exp1 and Exp2 in Figure S2, Table S1).

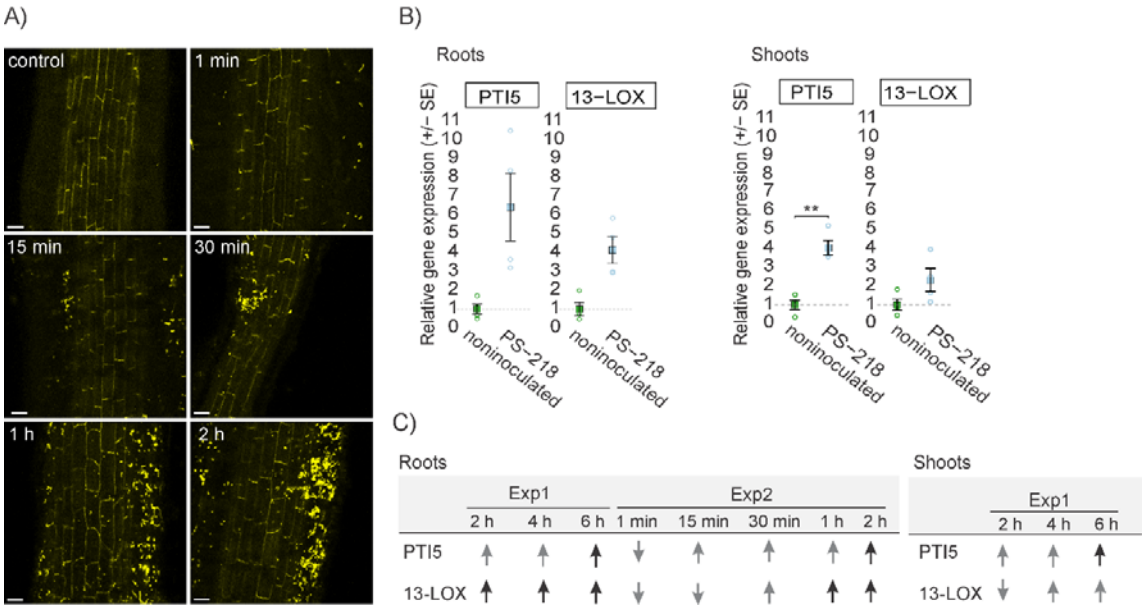

121

122 **Figure 1: Dynamics of biofilm formation and plant responses of potato to *B. subtilis*.** A) Biofilm formation (YFP
123 fluorescence) was followed on potato roots after incubation with *B. subtilis* PS-218 YFP for a specified time.
124 Scale is 50 µm. B) Potato response to bacteria colonization is robustly followed by expression of PTI5 and 13-
125 LOX. Relative expression of PTI5 and 13-LOX in roots and shoots of *B. subtilis* PS-218 YFP inoculated and non-
126 inoculated plants, after overnight incubation. Relative gene expression was scaled to the average gene
127 expression of non-inoculated group. Welch's t-test was used to determine differences between treatments.
128 Individual measurements (circles), mean (squares) and standard error are shown. Asterisks (*) denote a
129 statistically significant difference (p-value < 0.05). Data from all experiments are given in Table S1. C) Dynamics
130 of PTI5 and 13-LOX expression (up- or downregulation) in roots and shoots of potato plants after inoculation
131 with high *B. subtilis* strain PS-218 culture density (10^7 CFU/mL) and incubation for a specified time. Data of all
132 experiments are available in Table S1. Up- or downregulation was determined by comparing expression in
133 inoculated plants with expression in non-inoculated plants. ↑: upregulation, ↓: downregulation, **↑**:
134 statistically significant upregulation determined by Welch's t-test, **↓**: statistically significant downregulation
135 determined by Welch's t-test. Exp: experiment.

136

137 To study the dynamics of biofilm formation, we set up an experiment with higher density bacteria
138 inoculum (10^7 CFU/mL). In such set-up, biofilm reproducibly began forming after the first 15 minutes

139 of incubation, and it was consistently present over the entire root surface after a 2-hour incubation
140 period (Figure 1). Interestingly, the induction of PTI5 and 13-LOX genes was also detected when the
141 biofilm was formed uniformly on the root (Figure 1, Figure S2, Table S1).

142

143 **Complex regulatory network is triggered when potato is colonized with *B. subtilis***

144 To investigate plant response to *B. subtilis* colonization in more detail, we next performed RNA-seq
145 analysis of colonized roots and systemic shoot tissue. Our special interest was in the starting point of
146 colonization, as we intended to capture initial *B. subtilis* recognition related responses in the plant.
147 Therefore, roots were analyzed at the time of biofilm formation (2 hours post-inoculation (hpi)) and
148 24 hours later (26 hpi). The response of the plant was stronger at later time points (Figure 2A, Figure
149 S3). Moreover, shoots were analyzed at this later time to explore potential activation of MTI and/or
150 IR. For both root and shoot tissue, we identified a large overlap in differentially expressed genes for
151 plants inoculated with two different strains (Figure 2A, Figure S3).

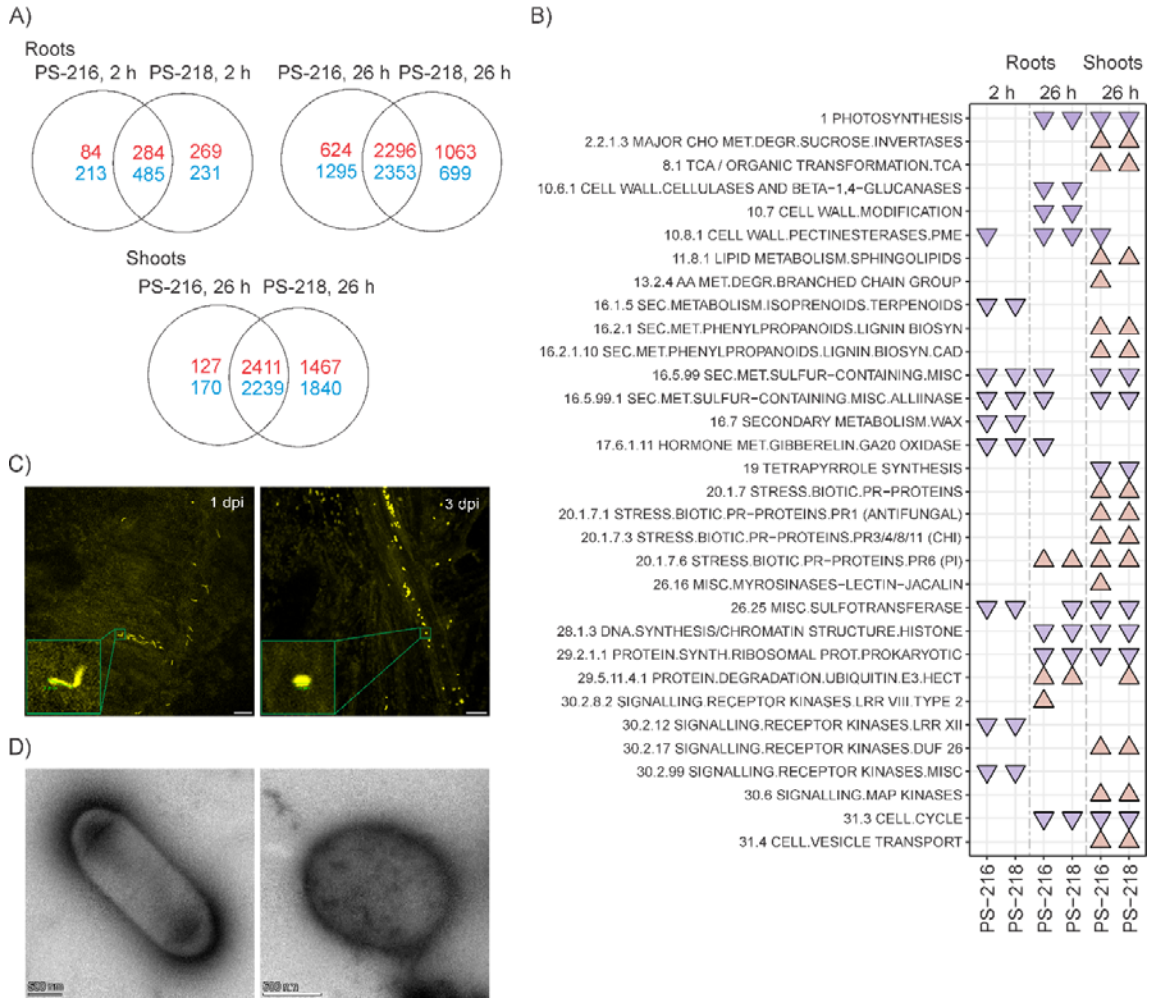

Figure 2: Potato adjusts to colonization with *B. subtilis* by repression of immune signaling and cell wall synthesis. A) Number of genes, regulated by *B. subtilis* in plant roots and shoots after 2-h and 26-h incubation with PS-216 YFP and PS-218 mKate2. Blue: downregulated genes, red: upregulated genes. B) Visualization of results in the context of biological pathways. For each comparison between *B. subtilis*-inoculated and non-inoculated plants, gene sets enriched for up- or downregulated genes (q-value < 0.1) are shown and designated as red triangles or blue triangles for shoots and roots at different time points. MapMan ontology BINs were used to generate gene sets. Sample group comparisons of inoculated to non-inoculated (in columns) are designated with bacterial strain names used for inoculation. PS-216: PS-216 YFP, PS-218: PS-218 mKate2. See Table S2 for all results. C) *B. subtilis* morphology is changed after internalization in plants. Left: *B. subtilis* morphology 1 dpi (day post-inoculation). Right: *B. subtilis* morphology 3 dpi. See Figure S4 for more data. Scale is 25 µm. D) Electron micrograph of free-living (left) and *in planta* living *B. subtilis* PS-216 (right). Scale is 500 nm.

166 Many processes related to primary line of defense were downregulated in roots at the time of
167 biofilm formation, including diverse immune receptors, genes involved in cell wall modifications and
168 in synthesis of terpenoids and waxes (Figure 2B). Interestingly, among the genes that were
169 upregulated in roots already at the time of biofilm formation were in majority genes coding for
170 transcription factors, hormonal synthesis, signalling components and components of protein
171 degradation. Several ERF transcription factors were upregulated besides the already identified PTI5,
172 as well as many MYBs, WRKYs, bZIP and NAC transcription factors. We also identified several
173 lipoxygenases upregulated (JA synthesis), but also genes involved in ethylene and gibberellin
174 synthesis as well as in Ca^{2+} signalling (Table S3). The response of most of these genes was intensified
175 in later time point in both roots and shoots (Table S3).

176 Remarkably, more induced gene sets were detected in shoots. The processes activated in shoots
177 resemble IR as studied so far in other plants. Receptor kinases were upregulated as were MAP
178 kinases and executors of plant defense, such as beta-glucanases, alpha amylase inhibitors, PR1
179 proteins and PR5 proteins (Figure 2B, Table S2, Table S3). Among the genes associated with
180 transcriptional regulation, NPR1 was also specifically upregulated in shoots only.

181 In addition, we also followed the extent of bacterial internalization within the plant. We detected
182 bacteria in stem already 1 day post-inoculation (dpi) (Figure S4). Interestingly, while plant responds
183 to *B. subtilis* colonization, also *B. subtilis* adapts once internalized as its morphology starts to change
184 to more rounded form as early as 2 dpi (Figure 2C, Figure S4). Also using electron microscopy, we can
185 see that most free-living bacteria are multiplying, while no multiplication was detected in *in planta*
186 living bacteria (Figure 2D, Figure S5).

187 **Biofilm formation and plant responses are attenuated in potato roots inoculated with *B. subtilis***
188 **quorum sensing and surfactin-deficient mutants**

189 To better understand the mechanisms that trigger plant responses, we inspected the role of the *B.*
190 *subtilis* ComX peptide mediated QS and surfactin production in potato–*B. subtilis* interaction. We

191 used two PS-216 mutant strains, one with deletion of the *comQXP* gene cluster, coding for the genes
192 involved in QS, which also regulate surfactin production (PS-216 Δ*comQXP*),[25] and the other strain
193 with a mutation in the *srfA* operon, which is unable to produce surfactin (PS-216 Δ*srfA mutant*). Both
194 mutants are reported to still form biofilms in liquid media.[34] The biofilm formed by both mutants on
195 potato root was barely detectable at 26 hours after inoculation, while strong biofilm formation was
196 observed for wild-type (WT) bacteria (Figure 3A, Figure S6, Table S4). The reduced ability to form
197 biofilm was also reflected in the potato response to *B. subtilis*. The induction of JA synthesis and
198 ethylene signalling markers observed in response to the WT was attenuated in the plant response to
199 the mutants. Similarly, the colonization associated downregulation of apoplastic ROS generator
200 RBOHD and photosynthesis marker CAB occurred to a lesser extent in response to the mutants
201 (Figure 3B, Table S5).

202

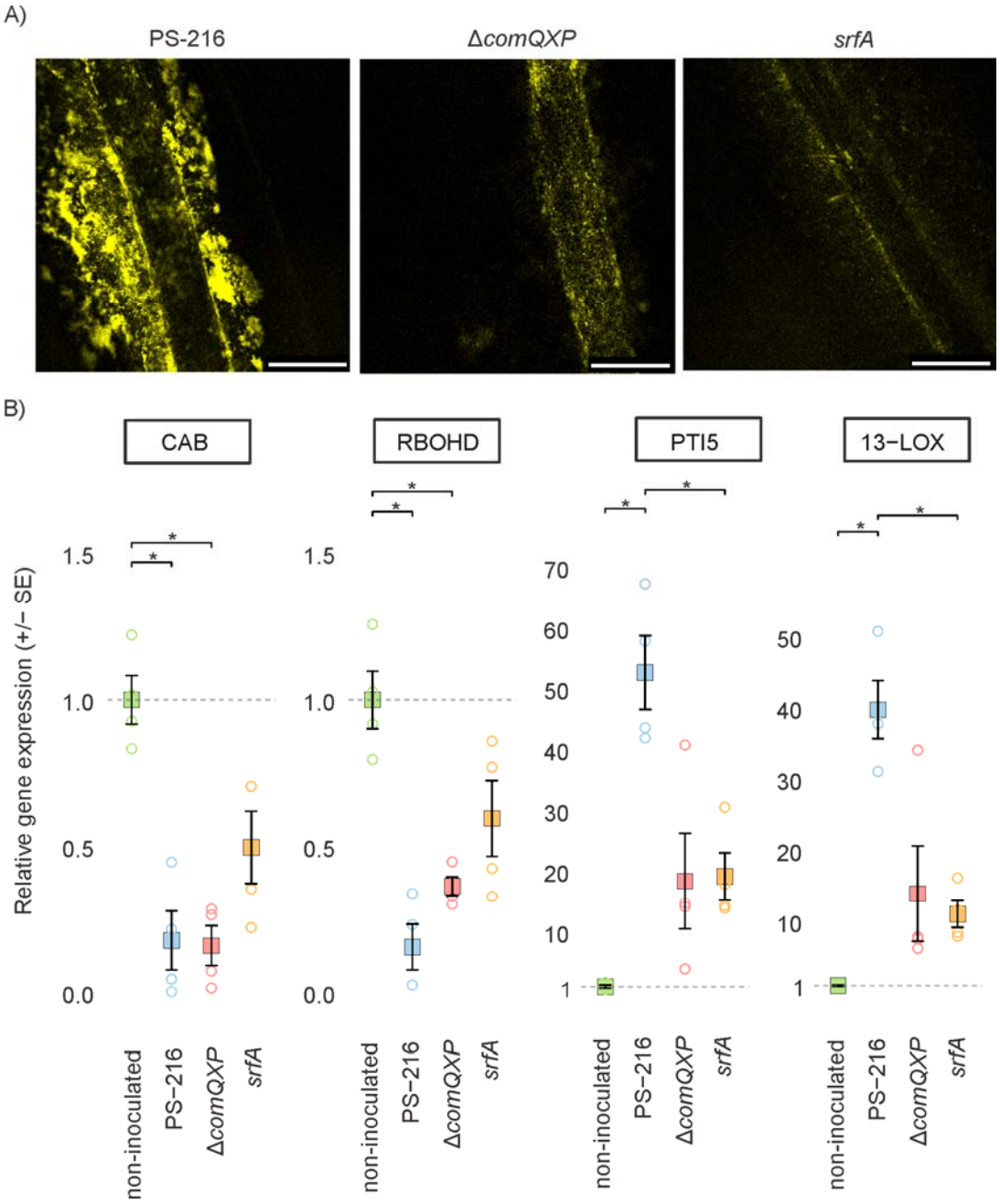

203

204 **Figure 3: Induction of plant responses is dependent on efficient *B. subtilis* biofilm formation on roots**. A)
205 Biofilm formation on potato roots after 26-h incubation with YFP-labelled *B. subtilis* PS-216 (left), quorum
206 sensing-negative *B. subtilis* YFP-labelled mutant PS-216 Δ*comQXP* (middle) and PS-216 srfA mutant (right)
207 culture. Scale is 500 µm. B) Expression of selected genes (RBOHD, 13-LOX, CAB, PTI5) in non-inoculated potato
208 roots and after 26-h incubation with *B. subtilis* PS-216 YFP, PS-216 Δ*comQXP* YFP and PS-216 *srfA* YFP. Relative
209 gene expression was scaled to the average gene expression of non-inoculated group. Welch's t-test was used to
210 determine differences between groups. Individual measurements (circles), mean (squares) and standard error

211 are shown. Asterisks (*) denote statistically significant difference (p-value < 0.05). See Table S5 for the results
212 of all genes for both roots and shoots.

213

214 To confirm that biofilm establishment is required for successful activation of plant responses, and
215 that *B. subtilis* secondary metabolites are not sufficient, we treated plants with the conditioned
216 media in which bacteria were growing. Results showed that the conditioned media alone did not
217 trigger any response in treated plants, albeit containing surfactin (Figure S7, Table S6). Therefore, we
218 conclude that *B. subtilis* biofilm formation on the roots is required for induction of potato response.

219

220 **Non-kin intraspecies interaction of *B. subtilis* strains on root intensifies potato responses**

221 To understand plant responses to colonizing bacterial communities, which is relevant for application
222 in practice, we set up an experiment inoculating plants with two genetically different, categorized
223 previously as non-kin, and two isogenic (only differently fluorescently labelled) *B. subtilis* strains.
224 When roots were inoculated with PS-216 and PS-218 strains separately, both equally colonized the
225 roots (Figure 4A, first two columns). Similarly, when differentially labelled isogenic strains were
226 combined, the resulting biofilm on the root contained similar abundances of each strain, with cells of
227 each strain spatially well mixed (Figure 4A, third column). On the other hand, when non-kin strains
228 PS-216 and PS-218 were combined, we observed biofilm with segregation of the two strains (Figure
229 4A, last column). Moreover, one of the strains dominated on the roots, with only a small amount of
230 biofilm formed by the other strain (Figure 4A, last column).

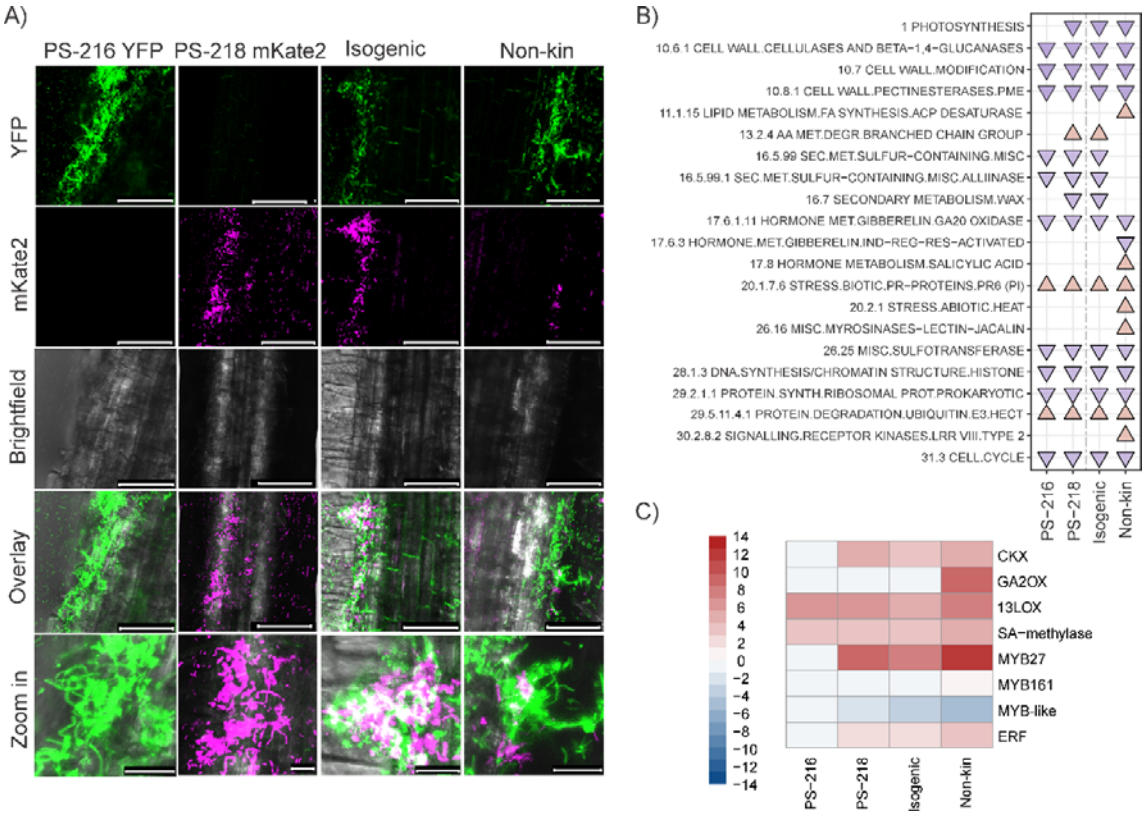

Figure 4: Social interactions of *B. subtillis* strains on potato roots intensify potato immune response. A) Colonization of potato roots by isogenic and non-kin *B. subtilis* strains after 4-h incubation. From top to bottom: YFP fluorescence, mKate2 fluorescence, brightfield, overlay of images, zoom in of overlay images. From left to right: PS-216 YFP, PS-218 mKate2, PS-218 YFP and PS-218 mKate2 (isogenic – self interaction), PS-216 YFP and PS-218 mKate2 (non-kin interaction). White color (overlay) shows colocalization of YFP and mKate2. The scale is 25 µm for **zoom in** images and 100 µm for all others. B) Visualization of responses in the context of biological pathways. For each comparison between *B. subtilis*-inoculated and non-inoculated plants, gene sets enriched for up- or downregulated genes (q-value < 0.1) are shown and designated as red triangles or blue triangles, respectively after 2-h incubation. MapMan ontology BINs were used to generate gene sets. Sample group comparisons to non-inoculated ones (in columns) are designated with bacterial strain names used for inoculation. PS-216: PS-216-YFP, PS-218: PS-218-mKate2, isogenic interaction: YFP-labelled PS-218 and mKate2-labelled PS-218, non-kin interaction: YFP-labelled PS-216 and mKate2-labelled PS-218. See Table S2 for all results. C) Examples of genes with intensified response when plant is interaction with two non-kin strains. Log2 values are shown. Blue: downregulated genes, red: upregulated genes, according to scale on the left.

We next performed RNA-seq analysis of roots at the time of uniform establishment of *B. subtilis* biofilm (2 hpi). In roots, the intensity of the transcriptional response to the non-kin strain mixture

249 was higher than that to the mixture of two isogenic, differentially labeled strains (Figure 4, Figure S3).
250 Regarding biological pathways, some receptor kinases (BINs 26.16 and 30.2.8.2) were specifically
251 upregulated in the non-kin interaction, as well as some enzymes from fatty acid biosynthesis (BIN
252 11.1.15) and heat shock proteins (BIN 20.2.1) (Figure 4B, Table S2). In addition, 422 genes had more
253 than 2-fold stronger response in the interaction with non-kin strains compared to monoculture or the
254 isogenic mixture. Among the more induced ones, are two MYB transcription factors, salicylate
255 carboxymethyltransferase, gibberellin 2-oxidase 2, peroxidase and beta-galactosidase genes (Table
256 S3).

257

258 ***B. subtilis* abundance is increased in plants with silenced PTI5**

259 We next overlayed data with plant stress signaling prior knowledge network, built from experimental
260 data on protein–protein interactions, protein–DNA interactions and metabolic pathways
261 (skm.nib.si).[35] The central signaling module that was regulated in the studied interaction was
262 ethylene signaling, linked to regulated JA synthesis, SA signaling and ROS signaling (Figure 5A; Figure
263 S8; Table S7). Thus, we focused on ERF transcription factors, as the role of ethylene signaling was so
264 far not in depth addressed in interaction of plants with beneficial microbes. Among ERFs, PTI5 was
265 found to be more than 50-fold induced when plants were exposed to *B. subtilis* monocultures or two-
266 strain mixtures, already early after colonization (after 2-hour incubation). This could indicate its role
267 as regulatory hub in plant colonization and/or biofilm formation. To test this role, we produced
268 transgenic potato with reduced expression of PTI5. First, we followed biofilm formation in transgenic
269 plants with silenced PTI5. Results showed that PTI5 is not involved in biofilm formation on roots
270 (Figure 5B, Table S8), as no difference in biofilm formation was detected between non-transgenic
271 (NT) and PTI5-silenced plants (Figure 5B, Figure S9, Table S8).

272

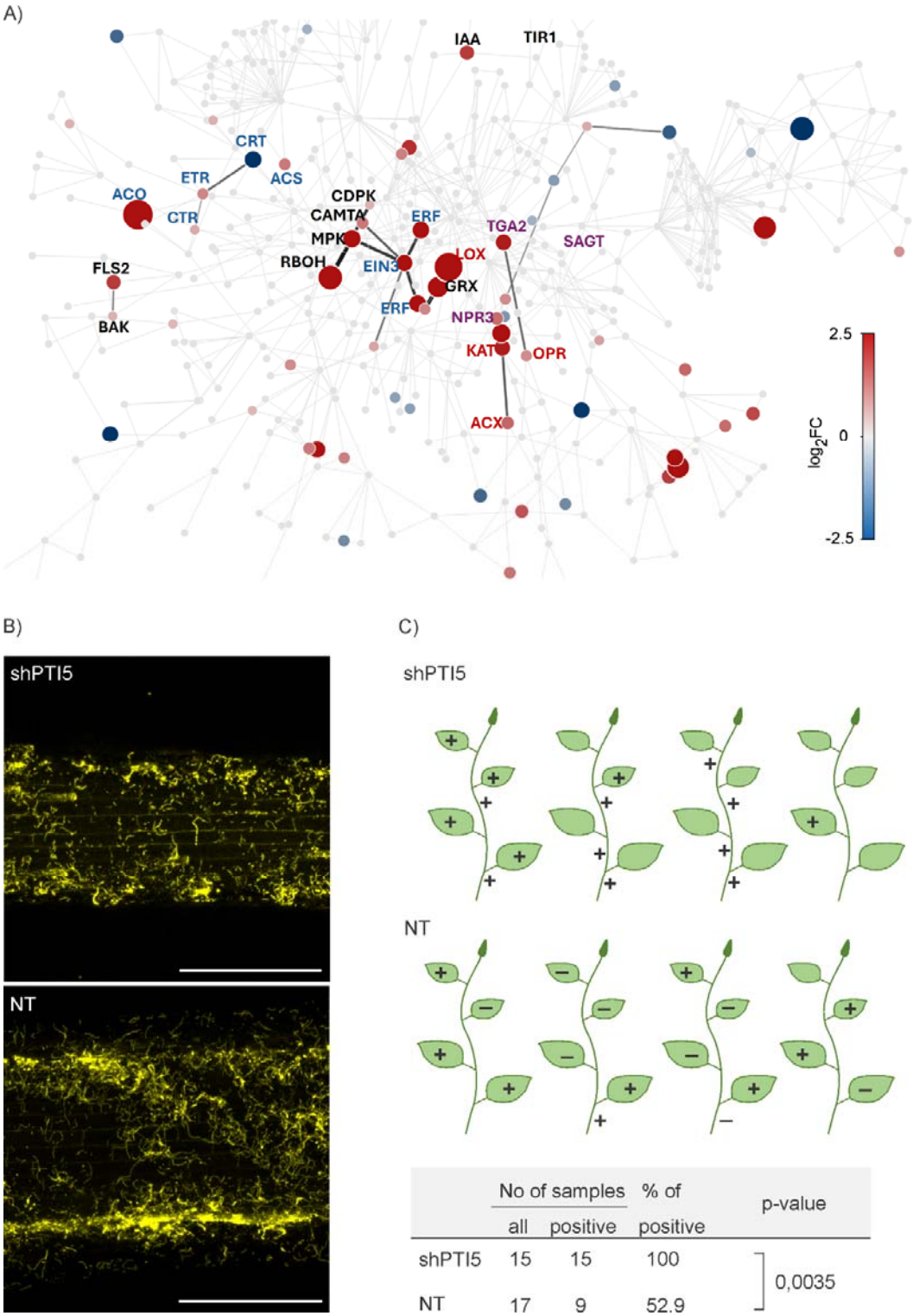

Figure 5: ERF transcription factor PTI5 is required for balanced colonization of potato plants. A) Plant immune signalling modules that were regulated following incubation of roots with non-kin mixture of *B. subtilis* strains. Genes and proteins are represented as nodes and interaction between them (protein–protein interaction, protein–DNA interaction) as edges of the network. Differentially expressed genes from ethylene (blue), JA

278 (red), SA (violoet) and other (black) signalling modules are shown. Black edge connected two differentially
279 expressed genes. All non-differentially expressed genes and edges are shown in grey. The size of the node
280 indicates the difference in expression between PS-216 and PS-218 inoculated and non-inoculated roots
281 (log2FC). See Table S7 for the name and description of regulated genes, and Figure S8 for information on
282 central signalling modules that were regulated in potato roots in isogenic interaction (PS-218 YFP + PS-218
283 mKate2). B) *B. subtilis* PS-218 YFP root colonization (yellow fluorescence) of transgenic potato with silenced
284 PTI5 (shPTI5) and non-transgenic potato plant (NT) after 2-h incubation. Scale is 250 µm. C) Bacillus abundance
285 in shPTI5 and NT potato plants. The scheme shows leaves of four shPTI5 and four NT plants in which the
286 presence of *B. subtilis* was (+) or was not (-) detected by qPCR in plants from soil which were incubated for 2 h
287 in PS-218 YFP before being planted and grown in soil for one week. Leaves with no mark were not analyzed.
288 The table presents a statistically significant difference in the percentage of positive samples (leaves, nodes and
289 internodes) between NT and shPTI5 plants determined by Fisher's exact test. See Table S9 for details. The
290 results of line L6 are shown and were confirmed on another transgenic line shPTI5 L2 (Figure S9, Table S10).

291

292 PTI5 was also upregulated in potato shoots. To test if it has a role in maintenance of *B. subtilis*
293 endophytic community we followed *B. subtilis* abundance in shoots of NT and PTI5-silenced plants. *B.*
294 *subtilis* abundance in systemic tissue was higher in PTI5-silenced plants, revealing that the balance in
295 the abundance of endophytic *B. subtilis* community was perturbed (Figure 5C, Table S9, Table S10).

296

297 **PTI5 is also regulating the extent of potato root colonization by arbuscular mycorrhizal fungi**

298 Considering the role of PTI5 in regulating endophytic colonization of *B. subtilis*, we aimed to explore
299 if this role was specific for this interaction or could be extended to other beneficial symbiosis. We
300 decided to explore the potential role of PTI5 in regulating the extension of root colonization by
301 arbuscular mycorrhizal fungi. This symbiosis is known to be under plant control to keep the
302 interaction under mutualistic levels and avoid excessive colonization.[36,37] With this aim, we explored
303 the colonization levels and symbiosis functionality in NT and PTI5-silenced lines. As shown in Figure 6,
304 *R. irregularis* successfully colonized potato roots, with intercellular hyphae, arbuscules and vesicles
305 present in the cortex. Remarkably, the extension of colonization, including the abundance of
306 arbuscules and vesicles was higher in the PTI5-silenced lines (Figure 6A). Indeed, the percentage of

307 root length colonized by the fungus was more than 2-fold higher in the silenced lines (Figure 6B), in
308 agreement with the higher amount of fungal DNA in those plants. To check if the functionality of the
309 mycorrhizal symbiosis was altered in those lines, we checked the expression levels of plant and
310 fungal transporters involved in the nutrient exchange between the symbionts within the arbuscules:
311 the potato phosphate transporter StPT4, and the fungal monosacharide transporter RiMST2, both
312 transcriptionally upregulated in arbusculated cells and defined as markers for symbiotic functionality
313 (Figure 6C). Both markers were upregulated in the PTI5-silenced lines, confirming the functionality of
314 the symbiosis.

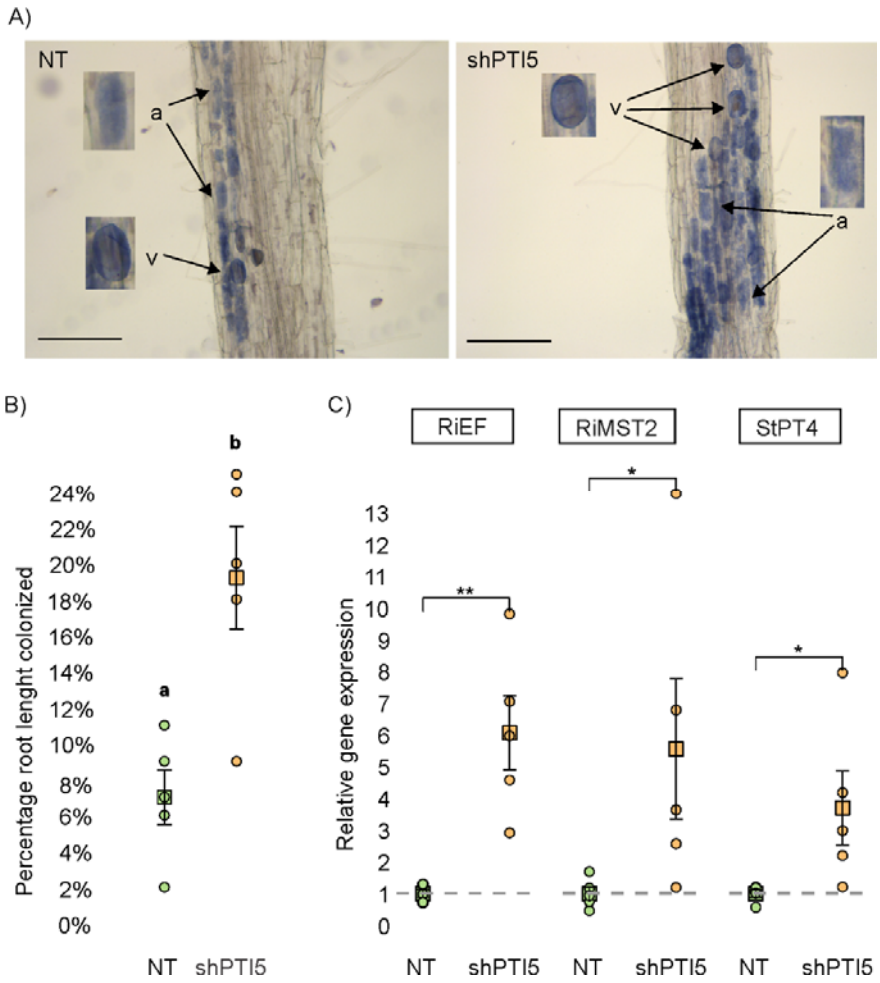

315

316 **Figure 6: Mycorrhizal colonization of potato roots in non-transgenic potato plant (NT) and PTI5-silenced**
317 **genotype (shPTI5).** A) Representative images of mycorrhizal colonization by *R. irregularis* in the different
318 genotypes. Fungal structures within the root cortex of potato plants are stained in blue (a: arbuscules, v:
319 vesicles). Scale is 200 µm. B) Percentage of root length colonized by the arbuscular mycorrhizal fungi *R.*

320 *irregularis*. C) Expression analysis of *R. irregularis* constitutive gene (RiEF) and symbiosis marker genes, the *R.*
321 *irregularis* monosaccharide transporter (RiMST2) and the potato phosphate transporter (StPT4), as well as
322 regression analysis using Dunn's pairwise comparisons were used to determine the differences between the
323 genotypes. Different letters show statistical differences. Permutation test was used to determine the
324 differences between the genotypes. Individual measurements (circles), mean (squares) and standard error are
325 shown. Asterisks denote a statistically significant difference (*: p-value < 0.05, **: p-value < 0.01). The results
326 of analysis of line L6 are shown and were confirmed on another transgenic line shPTI5 L2 (Figure S10).

327

328 **DISCUSSION**

329 Microbial inoculants have been proven as efficient and environmentally friendly alternatives to
330 chemical pesticides and fertilizers.[38,39] Current limitation in adopting such agricultural practices is
331 their variable efficiency in the field due to lack of understanding of mechanisms involved in the
332 regulation of plant colonization and maintenance of the plant microbiome.[6,40] Therefore, studying
333 the mechanisms regulating the interactions between crop plants and microbes is crucial to ensure
334 robustness of such plant protection approach. As the third most important crop in the world,
335 exceptionally sensitive to a wide range of stresses, potato is one of the most suitable candidates for
336 plant growth-promoting rhizobia (PGPR) based products.[31] We here established a model system for
337 such studies, exploring selected *B. subtilis* soil isolates individually or in mixtures. Furthermore, we
338 explored the potential extension of our findings by testing other widespread mutualistic interaction,
339 the arbuscular mycorrhizal symbiosis.

340 *B. subtilis* initially suppresses immune response in potato roots (e.g. downregulation of diverse
341 receptor kinases) thereby facilitating its own colonization, while it boosts induction of plant immunity
342 related genes in shoots at a later stage (Figure 2, Table S2), as it was shown also in other studies of
343 plants with beneficials as part of induced resistance phenomena.[13,41] Here we show that live bacteria
344 are required for triggering of the plant response, as the conditioned media in which bacteria were
345 growing did not trigger the response (Figure S7). Moreover, the intensity of the plant response was
346 dependent on the extent of biofilm formation on the potato root (Figure 3). Both, the mutant in

347 surfactin production and mutant in QS (also deficient in surfactin production) showed a reduced
348 ability to form biofilm on roots. This is interesting as the same strain was able to form floating
349 biofilms (pellicles),[42] suggesting that the ComX QS control of the biofilm development depends also
350 on plant factors. Besides residing on the plant roots, *B. subtilis* can also colonize the plant
351 endophytically. Internalised bacteria stop dividing and change the morphology (Figure 2, Figure S5).
352 The round bacterial form closely resembles L-form bacteria, which are characterized by modified or
353 absent cell walls.[42,43,44] We also tested the extent of bacteria internalisation with QS impaired strains,
354 which was interestingly not affected (Table S11).

355 To get insights into the complexity of plant–microbe interactions, we extended our studies to
356 application of two different *B. subtilis* strains to explore how bacterial diversity may influence the
357 plant response. We studied pairs of strains with different kin discrimination types of intraspecies
358 interactions — isogenic strains were predicted to be cooperative, and non-kin strains to be
359 antagonistic.[22] We observed that non-kin interaction of two *B. subtilis* strains invigorates the plant
360 response, especially in immune and abiotic signalling components (Figure 4, Table S3). These results
361 imply that even minor taxonomic changes in the phytobiome can lead to substantial differences in
362 the plant responses. Increasing evidence support that plants actively manage their microbiota for
363 balancing growth with immunity.[46] It has been reported that *B. subtilis* can promote plant growth via
364 direct pathways such as producing phytohormones (e.g., auxin, gibberellin, cytokinin, and abscisic
365 acid).[46,47,48] Both strains used in this study produce auxins (Table S12). Interestingly, we here show
366 that *B. subtilis* additionally regulates phytohormone metabolism *in planta*. Gibberellin 2-oxidase 2
367 and cytokinin oxidase, which catalyze the irreversible degradation of cytokinin and gibberellin
368 phytohormones, have been among the most induced genes by inoculation of non-kin *B. subtilis*
369 strains (Figure 4, Table S3). This could suggest that equilibrium between growth and immunity is
370 shifted towards immunity in plants inoculated by non-kin *B. subtilis* strains, as a functional relation
371 between lower activity of gibberellin signalling and reduced plant disease severity has previously
372 been confirmed in potato.[50] In accordance, indole-3-acetic acid-amido synthetase GH3.8 was in our

373 study induced in *B. subtilis* inoculated plants at late time point in both shoots and roots (Table S3).
374 GH3.8 functions as IAA-amino synthetase that prevents the accumulation of free indole acetic acid
375 (IAA), which increases plant disease resistance, growth and development.[51]

376 Not much is however known on the mechanisms that allow for successful colonisation of plants with
377 beneficial microbes while avoiding colonization by harmful pathogens. MTI is known to be induced
378 also when plant is exposed to beneficials.[11] In interaction of Arabidopsis with beneficial
379 *Pseudomonas* strain it was found that suberin biosynthesis is down regulated to allow for better
380 penetration of bacteria.[11] Similarly, in our study cell wall metabolism was downregulated in root
381 colonization (Figure 2, Figure 4). In addition, synthesis of toxic terpenoids was downregulated in
382 roots at the biofilm forming stage (Figure 2). Suppression of toxic ROS is crucial for successful
383 colonisation of plants by microbes.[24] We found ROS scavenger peroxidase and ROS generator RBOHD
384 induced and repressed, respectively, following inoculation by *B. subtilis* (Figure 3). Several studies
385 also reported the increase of peroxidase in different plant–*Bacillus* interactions, and in some cases
386 this induction have been associated to pathogen resistance.[51,52,53,54,55,56]

387 Plant colonisation is frequently linked to induction of SA, JA and ethylene signalling pathways and
388 transcriptional rewiring, of which MYB72, MYC2 and NPR1 transcription factors are the most studied
389 ones, and are proposed to be relevant for IR responses.[13,58] Here we found upregulation of the 13-
390 LOX pathway leading to JA synthesis, as previously described in other plant-PGPR interactions (Figure
391 1, Figure 3).[58,59,60] Similarly, several studies reported activation of SA signalling pathway.[14] We found
392 NPR1 upregulated in shoots (Table S2, Table S3). In corroboration with previous studies, we also
393 identified several MYB transcription factors induced in both roots and shoots (Table S3).

394 Modulation of ethylene signalling in plant microbiome interactions have been pinpointed as a central
395 element in their regulation and their impact on plant responses to stress.[62] For example, ethylene
396 have been proposed to regulate biofilm formation and root colonization by beneficial bacteria[63,64]
397 and the arbuscular mycorrhizal symbiosis,[65] and it is required for IR by beneficial bacteria and

398 fungi.[66,67] We also detected induction of the ethylene signalling pathway in *B. subtilis* inoculated
399 roots, including ETR, EIN3 and several ERF transcription factors (Figure 5, Figure S8, Table S3).
400 Moreover, 1-aminocyclopropane-1-carboxylate oxidase, which catalyzes the final step in ethylene
401 biosynthesis, was in our study induced in all tissue and time points, further suggesting involvement of
402 ethylene signalling pathway in potato response to *B. subtilis* (Figure 5, Figure S8, Table S3).
403 ERF transcription factors, the members of the AP2/ERF family active under ethylene signling, play
404 prominent roles in plant immunity, although the function of most of them remains unknown.[13,59,68,69]
405 A different set of ERFs was regulated in roots and shoots in our study. Among them, ERF transcription
406 factor PTI5 was strongly upregulated in all studied conditions. PTI5 was first identified in tomato as
407 interacting partner of the *R* gene *Pto* that confers resistance against the bacterial pathogen
408 *Pseudomonas syringae* pv. tomato.[70,71] On the other hand, we have previously shown that PTI5
409 negatively regulates potato defence response to pathogens potato virus Y and *Ralstonia*
410 *Solanacearum*, suggesting its role as susceptibility factor in potato immunity.[33] Interestingly, PTI5 is
411 transcriptionally regulated by EIN3 in the presence of SA only and on the protein level regulated by
412 autophagy degradation.[33] Results of this study suggest that PTI5 has a negative regulatory role also in
413 the maintenance of endophytic community in potato, as both *B. subtilis* abundance in systemic
414 tissues and mycorrhizal colonization of roots were increased in PTI5-silenced potato plants (Figure 5,
415 Figure 6). High PTI5 levels thus both increase susceptibility of potato to pathogens and reduce the
416 capability of plant to interact with beneficial organisms. PTI5 thus represents a target for future
417 breeding efforts leading towards sustainable potato production. Taking it altogether, we here set a
418 cornerstone in understanding how beneficial microbes and plant communicate to regulate
419 endophytic colonization and maintain mutualism and have identified a way for improved colonization
420 by beneficial through silencing of PTI5.
421
422
423

ACKNOWLEDGEMENTS

We thank Nastja Marondini, Anja Moškrič, Tina Koželj, Tim Godec, Ana Žuran and Olena Nesterenko for technical support and laboratory assistance. This research was financially supported by the Slovenian Research Agency grants P4-0165, P4-0116, J4-9302, J4-4550 and J4-3089, and grant MCIN/AEI/ PID2021-124813OBC31, "ERDF A way of making Europe" financed by the European Union.

AUTHOR CONTRIBUTIONS

Concept and design: TL, MJP, IMM, KG. Acquisition, analysis or interpretation of data: TL, BK, KP, KS, TGK, MZ, MP, PS, AV, VL, TMP, JMP, MJP, IMM, KG. Drafting of manuscript: TL, KG. Critical revision of the manuscript for important intellectual content: MZ, MP, PS, MJP, IMM, KG.

DECLARATION OF INTERESTS

The authors declare no competing interests.

METHODS

Plant material

Potato plants cv. Rywal (NT) and shPTI5-Rywal were grown in stem node tissue culture for two weeks after *in-vitro* micropropagation under controlled environmental conditions (22±2°C in the light and 19±2°C in the dark with 70–90 µmol/m2/s2 radiation (OSRAM L 58 W/77 FLUORA lamps, Germany) and a 16-h photoperiod) as previously explained.[72] For studying systemic *B. sublilis* spread, plants were planted in soil two weeks after node segmentation and grown under controlled environmental conditions for one week as previously described.[73] shPTI5-Rywal transgenic lines were prepared by introducing shPTI5 construct[33] into NT using *A. tumefaciens* LBA4404.[74] The transformed bacteria

447 were used for the transformation of NT stem internodes from *in vitro* plantlets as described in Lukan
448 et al.[73] using appropriate selection media.

449

450 ***B. subtilis* strains**

451 WT *B. subtilis* strains PS-216 and PS-218[75] tagged with red fluorescent protein (mKate2) and yellow
452 fluorescent protein (YFP) gene linked to a constitutive hyperspank promotor were used, namely PS-
453 218 *amyE::*$P_{hypercI03}$*-YFP* (Sp) (PS-218 YFP), PS-216 *amyE::*$P_{hypercI03}$*-YFP* (Sp) (PS-216 YFP), PS-218
454 *amyE::*$P_{hyperspank}$*-mKate2* (Chl) (PS-218 mKate2) and PS-216 *amyE::*$P_{hyperspank}$*-mKate2* (Chl) (PS-216
455 mKate2).[20,22] PS-216 mutants with impaired surfactin production PS-216 *amyE::PhypercI03-YFP* (Sp)
456 *srfA::Tn917 (mls)* (PS-216 *srfA* YFP)[22] and QS mutant PS-216 *ΔcomQXP::kan amyE::*$P_{hypercI03}$*-YFP* (Sp)
457 (PS-216 Δ*comQXP* YFP) (this work) were used. QS mutant PS-216 ΔcomQXP::kan amyE::PhypercI03-
458 YFP (Sp) was constructed by transformation of PS-216 amyE::PhypercI03-YFP (Sp)[22] with plasmid
459 pED302,[76] carrying a kanamycin cassette between *degQ* and *comA*, resulting in a deletion of the
460 *comQXP* locus.

461

462 **IAA production detection**

463 The production of IAA was assessed following the protocol of Pramanik et al.[77] Fresh bacterial
464 cultures were prepared from single colonies in LB medium supplemented with 0.1 % tryptophan and
465 incubated in the dark at 30°C with shaking at 120 rotations per minute (rpm) for 48 hours. After
466 incubation, cultures were centrifuged at 10,000 rpm for 5 minutes, and the supernatant was
467 transferred to a microtiter plate in triplicates. Equal volumes of Salkowski reagent (prepared by
468 adding 1 mL of 0.5 M ferric chloride to 50 mL of 35 % perchloric acid, mixed well, and stored in a
469 brown bottle) were added to each well. The mixture was incubated in the dark at room temperature
470 for 30 minutes. Blanks were prepared similarly, using only LB medium with 0,1 % tryptophan.

471 Absorbance was measured spectrophotometrically at 536 nm, and IAA concentrations were
472 calculated using a standard curve prepared with concentrations ranging from 10–100 µg/mL of IAA.

473 **Potato inoculation with *B. subtilis***

474 On day one, *B. subtilis* from permanent culture was plated on a solid LB medium with appropriate
475 (see methods section *B. subtilis* strains) antibiotics (100 µg/mL spectinomycin or 5 µg/mL
476 chloramphenicol) and incubated overnight at 37°C. On day two, a single colony was resuspended in 3
477 mL of LB medium with antibiotics and grown overnight at 200 rpm and 37°C. On day three at noon,
478 30 µL of the bacteria culture was inoculated in 3 mL of LB medium without antibiotic and grown for 3
479 hours at 200 rpm at 37°C (OD_{600} between 0.4 and 0.6). Bacterial culture was then diluted in 3 mL of
480 MS30 (5 g of Murashige and Skoog Basal Medium with vitamins and 30 g of sucrose per 1 L of
481 bidistilled water, pH 5.8) medium to OD_{600} 0.02.

482 For studying marker genes expression after potato incubation in bacterial culture of low density, two
483 weeks old potato plants from tissue cultures were added to diluted bacterial culture. Note that
484 diluted bacterial culture was incubated 16 hours at 11 rpm before adding potato plants. Shoots were
485 separated from the culture by parafilm cover and incubated for 21 hours at 11 rpm in a growth
486 chamber prior sampling for quantitative PCR (qPCR) (Exp1 and Exp2 in Figure S2). When studying if
487 the conditioned media triggered any response in treated plants (Table S6), plants were added to a
488 culture (shoots were separated from the culture by parafilm cover) and discarded after 17-hour
489 incubation. New plants were added to conditioned medium and incubated for 26 hours.

490 For studying *B. subtilis* morphology after internalization in plants, two weeks old potato plants in
491 tissue cultures grown in the solid MS30 medium were inoculated with 300 µL of bacterial culture,
492 which was spread on the medium and after a specified time (Figure S4), stem and leaves were
493 observed under confocal microscope.

494 In all other experiments, on day four in the morning (after 16-hour incubation), bacterial cultures
495 were vortexed, except when studying the role of QS and surfactin (Table S5, Table S6). Cultures of

496 different strains were mixed in a ratio of 1:1 when interactions were studied. In 3 mL of bacterial
497 cultures, two-week old potato plants from tissue cultures were added (shoots were separated from
498 the culture by parafilm cover) and incubated for a specified time (15 min to 26 hours), depending on
499 the experiment. When studying *B. subtilis* abundance in shPTI5 transgenic plants with qPCR (Table
500 S9, Table S10), plants were planted in soil after a 2-hour incubation. In all experiments, shoots were
501 not in contact with bacterial culture.

502

503 **Mycorrhizal symbiosis establishment and quantification**

504 The mycorrhizal inoculum was maintained as monoxenic culture consisting in an *in vitro* culture of
505 transformed carrot roots colonized by the arbuscular mycorrhizal fungus *R. irregularis* (MUCL 57021)
506 (REKA Group. B.V., Bleiswijk, The Netherlands), produced and maintained growing in Gel-Gro (ICN
507 Biochemicals, Aurora, OH, USA) as previously described in Chabot et al.[78] Potato plantlets growing in
508 125 mL pots with a mixture of soil, sand and vermiculite (3:2:1, v:v:v) were inoculated by adding a 1
509 cm piece of the monoxenic culture, containing approximately 50 *R. irregularis* spores, fungal hyphae
510 and colonized carrot roots. In the non-inoculated treatment, a piece of medium containing only
511 uninfected carrot roots was applied to the non-mycorrhizal controls. Plants were grown in a growth
512 chamber (day/night cycle: 16 h, 24°C/8 h, 19°C; relative humidity: 50 %). The experiment was
513 repeated twice and eight independent plants per genotype were analyzed.

514 Mycorrhizal colonization of roots and symbiosis establishment was evaluated histochemically and
515 molecularly mycorrhizal structures within the roots were observed and quantified after clearing the
516 roots in 10 % KOH and staining the fungal structures with 5 % black ink in 2 % acetic acid solution as
517 described in García at al.[79] Percentage of mycorrhizal colonization of roots was determined following
518 the gridline intersection method[80] using a Nikon SMZ1000 stereomicroscope. To quantify the total
519 amount of fungus within the root and assess symbiotic functionality we analysed the expression
520 levels of marker genes by qPCR (see below).

521

522

523 **Confocal microscopy**

524 Stellaris 8 Confocal microscope with HC PL FLUOTAR 10x/0.30 DRY objective (Leica Microsystems)
525 was used to detect emission of YFP and mKate2 on the roots of plants in the experiment for
526 investigating timing of biofilm formation, *B. subtilis* morphology after internalization in plants, biofilm
527 formation pattern when studying bacteria–plant social interactions, biofilm presence on the roots of
528 plants sampled for RNA-seq, biofilm formation in transgenic plants with silenced PTI5 and prior all
529 qPCR experiments to confirm roots colonization. Confocal microscope Leica TCS LSI macroscope with
530 Plan APO 5 x objective (Leica Microsystems) was used to detect emission of YFP when investigating
531 biofilm formation on the roots of mutants that have attenuated surfactin production. The emission
532 of YFP was followed after excitation with 488 nm laser in the window 505–560 nm. The emission of
533 mKate was followed after excitation with 589 nm laser in the window between 605–650 nm. Regions
534 of interest (ROI) were scanned unidirectionally with scan speed of 400 Hz and frame average at least
535 2. The images were processed to obtain maximum projections from Z-stacks for all channels and
536 merged using Leica LAS X software (Leica Microsystems). Mean intensity of fluorescence on confocal
537 images was determined in LAS X software (Leica). Statistically significant differences were
538 determined by Student's t-test.

539

540 **Transmission electron microscopy (TEM)**

541 Samples were prepared for examination with TEM using negative staining method. Pellets of
542 centrifuged liquid culture or leaf homogenate infiltrated with *B. subtilis* were resuspended in 0.1 M
543 phosphate buffer with 2 % polyvinylpyrrolidone. Six µL of resuspension was applied to copper grids
544 with or without glow discharge (400 mesh, formvar-carbon coated) for 5 minutes. Afterwards, the
545 remaining resuspension was dabbed with filter paper. This procedure was repeated two more times.

546 Afterwards, the grids were washed with bidistilled water and stained with one droplet of 1 % (w/v)
547 water solution of uranyl acetate. Two grids were prepared for each sample. The grids were observed
548 by transmission electron microscope TALOS L120 (ThermoFisher SCIENTIFIC, The Netherlands),
549 operating at 100 kV and representative micrographs were acquired (camera Ceta 16M) using Velox
550 software.
551

552 **qPCR analysis**

553 The shoots and elongation zones of roots of *B. subtilis*-inoculated and non-inoculated (see
554 description of inoculation chapter) potato plants were sampled in four or five biological replicates
555 (plants). RNA was isolated by RNeasy Plant Mini Kit (Qiagen) from shoots and RNeasy Plant Mini Kit
556 (Qiagen) or RNeasy Micro Kit (Qiagen) from roots according to the manufacturer's protocols.
557 Concentration and purity of DNase-treated (0.5 µL of DNase I per µg RNA; Qiagen) total RNA was
558 evaluated using NanoDrop ND1000 spectrophotometer (Nanodrop technologies) and agarose gel
559 electrophoresis and then reverse-transcribed using the High-Capacity cDNA Reverse Transcription Kit
560 (Thermo Fisher Scientific) or High-Capacity RNA-to-cDNA Kit (Thermo Fisher Scientific). To determine
561 *B. subtilis* abundance in systemic shoot tissue, genomic DNA was isolated by MagMAX™ Plant DNA
562 Isolation Kit (Thermo Fisher Scientific) according to the manufacturer's protocol. Concentration and
563 purity were evaluated as stated above.

564 Samples were analyzed in the setup for qPCR as previously described.[32] The expression of 8 genes
565 (RBOHD, HSP70, PTI5, 13-LOX, PR1B, BGLU2, CPI8, CAB) involved in different steps of immune
566 signaling (Table S13 for a full list of genes and their description) was determined and normalized to
567 the expression of two validated reference genes, COX and elongation factor 1 (EF-1), as described
568 previously.[81] See Lukan et al.[32] for primer and probe information. Relative copy numbers of *comQ*
569 from *B. subtilis* were determined and normalized to relative copy numbers of NPR1 (a single copy

570 gene, https://spuddb.uga.edu/). The standard curve method was used for relative gene expression
571 quantification using quantGenius (http://quantgenius.nib.si).[82]
572 For molecular assessment of mycorrhizal colonization, the expression of the constitutive *R.*
573 *irregularis* elongation factor 1 (RiEF) gene and the markers of symbiotic functionality, the fungal
574 RiMST2 and the plant StPT4, both involved in the nutrient exchange between the symbionts in the
575 arbuscules were determined in roots by qPCR using gene-specific primers (Table S13). Relative
576 quantification of specific mRNA levels was performed using the comparative 2-Δ(ΔCt) method.[83]
577 Expression values were normalized using the normalizer gene EF-1α encoding the potato translation
578 elongation factor-1α. [84] Five independent biological replicates per treatment were analyzed.
579 Statistical analysis was conducted in R version 4.3.1.[85] Relative gene expression was scaled to the
580 average relative gene expression of the non-inoculated group.[86] Mean, standard deviation, standard
581 error of the mean and 95 % confidence intervals were calculated per gene, tissue type and genotype
582 and visualised using the ggplot2 package v3.3.6.[87] Pairwise Welch's t-test with holm correction for
583 multiple testing adjustment was employed to quantify the difference between the groups. Results
584 were visualised using rstatix v0.7.0[88] and ggpubr v0.4.0[89] R packages.
585
586 **RNA-seq analysis**
587 RNA was isolated from shoots and elongation zones of roots by RNeasy Plant Mini Kit (Qiagen) and
588 treated with RNA Clean & Concentrator-5 (DNase Included) (Zymo Research). In RNA-seq Exp 1, RNA-
589 seq was for roots performed after 2- and 26-hours incubations with *B. subtilis* culture and for shoots
590 after 26 hours of incubation, both for monocultures (PS-216 YFP, PS-218 YFP) and non-inoculated
591 samples (incubation in MS30 medium) as a control. In RNA-seq Exp 2, RNA-seq was for roots
592 performed after 2 hours of incubation with *B. subtilis* culture for monocultures (PS-216 YFP, PS-218
593 YFP, PS-218 mKate2), isogenic mixture (PS-218 mKate2 + PS-218 YFP), non-kin mixture (PS-218
594 mKate2 + PS-216 YFP) and non-inoculated samples (incubation in MS30 medium) as a control. Four
595 biological replicates (plants) were analyzed for each interaction (Table S14).

596 Raw paired-end Illumina reads were adapter-trimmed and reads below average PHRED basecall
597 quality score 20 were removed using Trim Galore (https://github.com/FelixKrueger/TrimGalore).[90]
598 Sequencing quality control was performed using FastQC v0.11.9.[91] Taxonomic classification of reads
599 was performed using Centrifuge v1.0.4[92] in conjunctions with the 2018 nt database. Reads were
600 mapped to *Solanum tuberosum* Phureja clone DM 1-3 genome with STAR v2.7.5c[93] using the merged
601 genome annotations GFF3.[94] Only uniquely mapped fragments were counted (--
602 outFilterMultimapNmax 1) and additional alignment parameters were set to restrict erroneous
603 mapping (--outFilterMismatchNoverReadLmax 0.02, --quantTranscriptomeBan Singleend, --
604 outFilterType BySJout, --alignSJoverhangMin 10, --alignSJDBoverhangMin 1, --alignIntronMin 20, --
605 alignIntronMax 10000, --alignMatesGapMax 10000). Centrifuge and mapping results showed
606 substantial contamination of sample BS472, therefore we excluded this sample from further analysis.

607 Gene Set Enrichment Analysis[95] was performed using MapMan[96] based gene sets (gmt file available
608 at https://github.com/nib-si/ptda)[97] and non-filtered normalized read counts, comparing different
609 Bacillus treatments to non-inoculated plants to identify significantly altered regulation of processes
610 and functionally related gene groups (FDR corrected q-value < 0.10). Results of all GSEA comparisons
611 were merged using R v4.3.1.[85] GSEA figure was generated using adjusted gseaFromStats function
612 from biokit v0.1.1 package.[98]

613 Differential gene expression analysis was performed in R using the *limma* package.[99] Low expressed
614 genes were filtered by retaining only genes with raw read counts above 100 in at least 11 samples for
615 RNA-seq Exp 2 and above 50 counts in at least 4 samples for RNA-seq Exp 1. Root and leaf samples
616 were analyzed separately. Normalized counts were transformed using voom function, followed by
617 linear model fit, and statistics calculation for defined contrasts using the eBayes function. Genes with
618 Benjamini-Hochberg FDR adjusted p-values < 0.05 and $|\log_2 FC| > 1$ were considered significantly
619 differentially expressed. Venn diagrams were plotted using a modified limma::vennDiagram function.

620 Raw and normalized read counts were deposited in GEO under accession number GSE232028.
621 Results of RNA-seq were validated by qPCR (Table S1).

622

623 **Network analysis**

624 Mechanistic Plant Stress Signalling (PSS) (https://skm.nib.si/)[35] reaction network was pre-processed
625 using DiNARs'[100] pre-processing app. Interactions among different molecular entities (such as genes,
626 proteins or transcripts) are defined on functional cluster level, mostly encompassed of *A. thaliana*
627 gene identifiers. Therefore, *Solanum tuberosum* gene identifiers[94] were first translated to Arabidopsis
628 gene identifiers using BLAST+ reciprocal best hit (RBH) search[101] on proteomes (file available at
629 https://github.com/NIB-SI/DiNAR/tree/master/TranslationTables). Top three potato identifiers per
630 Arabidopsis identifier were considered and further prioritised to the functinal cluster using DiNARs'
631 prioritisation script. Experimental data were superimposed onto the PSS network and visualised
632 using DiNAR. Separate condition specific networks, as defined by differential expression contrasts,
633 were exported as individual interactive .html files for further examination.

634

635 **REFERENCES**

636 1. Mauchline, T.H., and Malone, J.G. (2017). Life in earth – the root microbiome to the rescue?
637 Curr Opin Microbiol *37*, 23–28. https://doi.org/10.1016/j.mib.2017.03.005.

638 2. Timmusk, S., Behers, L., Muthoni, J., Muraya, A., and Aronsson, A.C. (2017). Perspectives and
639 challenges of microbial application for crop improvement. Front Plant Sci *8*.
640 https://doi.org/10.3389/fpls.2017.00049.

641 3. Pozo, M.J., Zabalgogeazcoa, I., Vazquez de Aldana, B.R., and Martinez-Medina, A. (2021).
642 Untapping the potential of plant mycobiomes for applications in agriculture. Curr Opin Plant
643 Biol *60*. https://doi.org/10.1016/j.pbi.2021.102034.

644 4. Kandel, S.L., Joubert, P.M., and Doty, S.L. (2017). Bacterial endophyte colonization and
645 distribution within plants. Microorganisms *5*.
646 https://doi.org/10.3390/microorganisms5040077.

647 5. O'Callaghan, M., Ballard, R.A., and Wright, D. (2022). Soil microbial inoculants for sustainable
648 agriculture: Limitations and opportunities. Soil Use Manag *38*, 1340–1369.
649 https://doi.org/10.1111/sum.12811.

650 6. Lutz, S., Bodenhausen, N., Hess, J., Valzano-Held, A., Waelchli, J., Deslandes-Hérold, G.,
651 Schlaeppi, K., and van der Heijden, M.G.A. (2023). Soil microbiome indicators can predict crop
652 growth response to large-scale inoculation with arbuscular mycorrhizal fungi. Nat Microbiol *8*,
653 2277–2289. https://doi.org/10.1038/s41564-023-01520-w.

654 7. Ngou, B.P.M., Ding, P., and Jones, J.D.G. (2022). Thirty years of resistance: Zig-zag through the
655 plant immune system. Plant Cell *34*, 1447–1478. https://doi.org/10.1093/plcell/koac041.

656 8. Baebler, Š., Witek, K., Petek, M., Stare, K., Tušek-Žnidarič, M., Pompe-Novak, M., Renaut, J.,
657 Szajko, K., Strzelczyk-Zyta, D., Marczewski, W., et al. (2014). Salicylic acid is an indispensable
658 component of the Ny-1 resistance-gene-mediated response against Potato virus y infection in
659 potato. J Exp Bot *65*, 1095–1109. https://doi.org/10.1093/jxb/ert447.

660 9. Tsai, H.H., Wang, J., Geldner, N., and Zhou, F. (2023). Spatiotemporal control of root immune
661 responses during microbial colonization. Curr Opin Plant Biol *74*.
662 https://doi.org/10.1016/j.pbi.2023.102369.

663 10. Teixeira, P.J.P.L., Colaianni, N.R., Law, T.F., Conway, J.M., Gilbert, S., Li, H., Salas-González, I.,
664 Panda, D., Risco, N.M. Del, Finkel, O.M., et al. (2021). Specific modulation of the root immune
665 system by a community of commensal bacteria. Proc Natl Acad Sci U S A *118*.
666 https://doi.org/10.1073/pnas.2100678118.

667 11. Verbon, E.H., Liberman, L.M., Zhou, J., Yin, J., Pieterse, C.M.J., Benfey, P.N., Stringlis, I.A., and
668 de Jonge, R. (2023). Cell-type-specific transcriptomics reveals that root hairs and endodermal
669 barriers play important roles in beneficial plant-rhizobacterium interactions. Mol Plant *16*,
670 1160–1177. https://doi.org/10.1016/j.molp.2023.06.001.

671 12. De Kesel, J., Conrath, U., Flors, V., Luna, E., Mageroy, M.H., Mauch-Mani, B., Pastor, V., Pozo,
672 M.J., Pieterse, C.M.J., Ton, J., et al. (2021). The Induced Resistance Lexicon: Do's and Don'ts.
673 Trends Plant Sci *26*, 685–691. https://doi.org/10.1016/j.tplants.2021.01.001.

674 13. Pieterse, C.M.J., Zamioudis, C., Berendsen, R.L., Weller, D.M., Van Wees, S.C.M., and Bakker,
675 P.A.H.M. (2014). Induced systemic resistance by beneficial microbes. Annu Rev Phytopathol
676 *52*, 347–375. https://doi.org/10.1146/annurev-phyto-082712-102340.

677 14. Yu, Y., Gui, Y., Li, Z., Jiang, C., Guo, J., and Niu, D. (2022). Induced Systemic Resistance for
678 Improving Plant Immunity by Beneficial Microbes. Plants *11*.
679 https://doi.org/10.3390/plants11030386.

680 15. Fiorilli, V., Martínez-Medina, A., Pozo, M.J., and Lanfranco, L. (2024). Plant Immunity
681 Modulation in Arbuscular Mycorrhizal Symbiosis and Its Impact on Pathogens and Pests. Annu
682 Rev Phytopathol *62*, 127–156. https://doi.org/10.1146/annurev-phyto-121423-042014.

683 16. Flemming, H.C., Wingender, J., Szewzyk, U., Steinberg, P., Rice, S.A., and Kjelleberg, S. (2016).
684 Biofilms: An emergent form of bacterial life. Nat Rev Microbiol *14*, 563–575.
685 https://doi.org/10.1038/nrmicro.2016.94.

686 17. Mitri, S., and Richard Foster, K. (2013). The genotypic view of social interactions in microbial
687 communities. Annu Rev Genet *47*, 247–273. https://doi.org/10.1146/annurev-genet-111212-
688 133307.

689 18. Asfahl, K.L., and Schuster, M. (2017). Social interactions in bacterial cell-cell signaling. FEMS
690 Microbiol Rev *41*, 92–107. https://doi.org/10.1093/femsre/fuw038.

691 19. Kalamara, M., Spacapan, M., Mandic-Mulec, I., and Stanley-Wall, N.R. (2018). Social
692 behaviours by Bacillus subtilis: quorum sensing, kin discrimination and beyond. Mol Microbiol
693 *110*, 863–878. https://doi.org/10.1111/mmi.14127.

694 20. Stefanic, P., Kraigher, B., Lyons, N.A., Kolter, R., and Mandic-Mulec, I. (2015). Kin
695 discrimination between sympatric Bacillus subtilis isolates. Proc Natl Acad Sci U S A *112*,
696 14042–14047. https://doi.org/doi.org/10.1073/pnas.1512671112.

697 21. Lyons, N.A., Kraigher, B., Stefanic, P., Mandic-Mulec, I., and Kolter, R. (2016). A combinatorial
698 kin discrimination system in Bacillus subtilis. Current Biology *26*, 733–742.
699 https://doi.org/10.1016/j.cub.2016.01.032.

700 22. Kraigher, B., Butolen, M., Stefanic, P., and Mandic Mulec, I. (2022). Kin discrimination drives
701 territorial exclusion during Bacillus subtilis swarming and restrains exploitation of surfactin.
702 ISME Journal *16*, 833–841. https://doi.org/10.1038/s41396-021-01124-4.

703 23. Lareen, A., Burton, F., and Schäfer, P. (2016). Plant root-microbe communication in shaping
704 root microbiomes. Plant Mol Biol *90*, 575–587. https://doi.org/10.1007/s11103-015-0417-8.

705 24. Liu, Y., Xu, Z., Chen, L., Xun, W., Shu, X., Chen, Y., Sun, X., Wang, Z., Ren, Y., Shen, Q., et al.
706 (2024). Root colonization by beneficial rhizobacteria. FEMS Microbiol Rev *48*.
707 https://doi.org/10.1093/femsre/fuad066.

708 25. Oslizlo, A., Stefanic, P., Dogsa, I., and Mandic-Mulec, I. (2014). Private link between signal and
709 response in Bacillus subtilis quorum sensing. Proc Natl Acad Sci U S A *111*, 1586–1591.
710 https://doi.org/10.1073/pnas.1316283111.

711 26. Ongena, M., Jourdan, E., Adam, A., Paquot, M., Brans, A., Joris, B., Arpigny, J.L., and Thonart,
712 P. (2007). Surfactin and fengycin lipopeptides of Bacillus subtilis as elicitors of induced
713 systemic resistance in plants. Environ Microbiol *9*, 1084–1090.
714 https://doi.org/10.1111/j.1462-2920.2006.01202.x.

715 27. López, D., Fischbach, M.A., Chu, F., Losick, R., and Kolter, R. (2009). Structurally diverse natural
716 products that cause potassium leakage trigger multicellularity in Bacillus subtilis. Proc Natl
717 Acad Sci U S A *106*, 280–285. https://doi.org/doi/10.1073/pnas.0810940106.

718 28. Danevčič, T., Dragoš, A., Spacapan, M., Stefanic, P., Dogsa, I., and Mandic-Mulec, I. (2021).
719 Surfactin Facilitates Horizontal Gene Transfer in Bacillus subtilis. Front Microbiol *12*.
720 https://doi.org/10.3389/fmicb.2021.657407.

721 29. Rahman, F. Bin, Sarkar, B., Moni, R., and Rahman, M.S. (2021). Molecular genetics of surfactin
722 and its effects on different sub-populations of Bacillus subtilis. Biotechnology Reports *32*.
723 https://doi.org/10.1016/j.btre.2021.e00686.

724 30. Chaudhry, V., Runge, P., Sengupta, P., Doehlemann, G., Parker, J.E., and Kemen, E. (2021).
725 Shaping the leaf microbiota: Plant-microbe-microbe interactions. J Exp Bot *72*, 36–56.
726 https://doi.org/10.1093/jxb/eraa417.

727 31. Vilvert, E., Stridh, L., Andersson, B., Olson, Å., Aldén, L., and Berlin, A. (2022). Evidence based
728 disease control methods in potato production: a systematic map protocol. Environ Evid *11*.
729 https://doi.org/10.1186/s13750-022-00259-x.

730 32. Lukan, T., Pompe-Novak, M., Baebler, Š., Tušek-Žnidarič, M., Kladnik, A., Križnik, M., Blejec, A.,
731 Zagorščak, M., Stare, K., Dušak, B., et al. (2020). Precision transcriptomics of viral foci reveals
732 the spatial regulation of immune-signaling genes and identifies RBOHD as an important player
733 in the incompatible interaction between potato virus Y and potato. Plant Journal *104*, 645–
734 661. https://doi.org/10.1111/tpj.14953.

735 33. Coll, A., Lukan, T., Stare, K., Zagorščak, M., Mahkovec Povalej, T., Baebler, Š., Prat, S., Coll,
736 N.S., Valls, M., Petek, M., et al. (2024). The StPti5 ethylene response factor acts as a
737 susceptibility factor by negatively regulating the potato immune response to pathogens. New
738 Phytologist *244*, 202–218. https://doi.org/10.1111/nph.20004.

739 34. Thérien, M., Kiesewalter, H.T., Auria, E., Charron-Lamoureux, V., Wibowo, M., Maróti, G.,
740 Kovács, Á.T., and Beauregard, P.B. (2020). Surfactin production is not essential for pellicle and
741 root-associated biofilm development of Bacillus subtilis. Biofilm *2*.
742 https://doi.org/10.1016/j.bioflm.2020.100021.

743 35. Bleker, C., Ramšak, Ž., Bittner, A., Podpečan, V., Zagorščak, M., Wurzinger, B., Baebler, Š.,
744 Petek, M., Križnik, M., van Dieren, A., et al. (2024). Stress Knowledge Map: A knowledge graph
745 resource for systems biology analysis of plant stress responses. Plant Commun *5*.
746 https://doi.org/10.1016/j.xplc.2024.100920.

747 36. Lidoy, J., López-García, Á., Amate, C., García, J.M., Flors, V., García-Garrido, J.M., Azcón-
748 Aguilar, C., López-Raez, J.A., and Pozo, M.J. (2023). Regulation of mycorrhizal colonization
749 under stress in tomato depends on symbiotic efficiency. Environ Exp Bot *215*.
750 https://doi.org/10.1016/j.envexpbot.2023.105479.

751 37. Ho-Plágaro, T., and García-Garrido, J.M. (2022). Molecular Regulation of Arbuscular
752 Mycorrhizal Symbiosis. Int J Mol Sci *23*. https://doi.org/10.3390/ijms23115960.

753 38. Alves de Andrade, L., Santos, C.H.B., Frezarin, E.T., Sales, L.R., and Rigobelo, E.C. (2023). Plant
754 Growth-Promoting Rhizobacteria for Sustainable Agricultural Production. Microorganisms *11*.
755 https://doi.org/10.3390/microorganisms11041088.

756 39. Minchev, Z., Ramírez-Serrano, B., Dejana, L., Lee Díaz, A.S., Zitlalpopoca-Hernandez, G., Orine,
757 D., Saha, H., Papantoniou, D., García, J.M., González-Céspedes, A., et al. (2024). Beneficial soil
758 fungi enhance tomato crop productivity and resistance to the leaf-mining pest Tuta absoluta
759 in agronomic conditions. Agron Sustain Dev *44*. https://doi.org/10.1007/s13593-024-00991-3.

760 40. Tsotetsi, T., Nephali, L., Malebe, M., and Tugizimana, F. (2022). Bacillus for Plant Growth
761 Promotion and Stress Resilience: What Have We Learned? Plants *11*.
762 https://doi.org/10.3390/plants11192482.

763 41. Blake, C., Christensen, M.N., and Kovacs, A.T. (2021). Molecular aspects of plant growth
764 promotion and protection by Bacillus subtilis. Molecular Plant-Microbe Interactions *34*, 15–
765 25. https://doi.org/10.1094/MPMI-08-20-0225-CR.

766 42. Špacapan, M., Danevčič, T., Štefanic, P., Porter, M., Stanley-Wall, N.R., and Mandic-Mulec, I.
767 (2020). The ComX quorum sensing peptide of Bacillus subtilis affects biofilm formation

768 negatively and sporulation positively. Microorganisms *8*.
769 https://doi.org/10.3390/microorganisms8081131.

770 43. Allan, E.J., Hoischen, C., and Gumpert, J. (2009). Chapter 1 Bacterial L-Forms
771 https://doi.org/10.1016/S0065-2164(09)01201-5.

772 44. Leaver, M., Domínguez-Cuevas, P., Coxhead, J.M., Daniel, R.A., and Errington, J. (2009). Life
773 without a wall or division machine in Bacillus subtilis. Nature *457*, 849–853.
774 https://doi.org/10.1038/nature07742.

775 45. Daulagala, P.W.H.K.P. (2021). Association of L-form Bacteria with Plants and their Application
776 in Biological Control of Phytopathogenic Fungi and Bacteria: A Review. J Adv Microbiol *21*, 77–
777 86. https://doi.org/10.9734/jamb/2021/v21i1030395.

778 46. Ku, Y.S., Liao, Y.J., Chiou, S.P., Lam, H.M., and Chan, C. (2024). From trade-off to synergy:
779 microbial insights into enhancing plant growth and immunity. Plant Biotechnol J *22*, 2461–
780 2471. https://doi.org/10.1111/pbi.14360.

781 47. Karadeniz, A., Topcuo?lu, Ş.F., and Inan, S. (2006). Auxin, gibberellin, cytokinin and abscisic
782 acid production in some bacteria. World J Microbiol Biotechnol *22*, 1061–1064.
783 https://doi.org/10.1007/s11274-005-4561-1.

784 48. Hamdache, A., Lamarti, A., Aleu, J., and Collado, I.G. (2011). Non-peptide metabolites from
785 the genus Bacillus. J Nat Prod *74*, 893–899. https://doi.org/10.1021/np100853e.

786 49. Gamalero, E., and Glick, B.R. (2011). Chapter 2 Mechanisms Used by Plant Growth-Promoting
787 Bacteria D. K. Maheshwari, ed. (Springer) https://doi.org/10.1007/978-3-642-21061-7_2.

788 50. Križnik, M., Petek, M., Dobnik, D., Ramšak, Ž., Baebler, Š., Pollmann, S., Kreuze, J.F., Žel, J., and
789 Gruden, K. (2017). Salicylic acid perturbs sRNA-gibberellin regulatory network in immune
790 response of potato to potato virus Y infection. Front Plant Sci *8*.
791 https://doi.org/10.3389/fpls.2017.02192.

792 51. Xu, G., Zhang, Y., Li, M., Jiao, X., Zhou, L., and Ming, Z. (2021). Crystal structure of the acyl acid
793 amido synthetase GH3-8 from Oryza sativa. Biochem Biophys Res Commun *534*, 266–271.
794 https://doi.org/10.1016/j.bbrc.2020.11.098.

795 52. Chowdappa, P., Mohan Kumar, S.P., Jyothi Lakshmi, M., and Upreti, K.K. (2013). Growth
796 stimulation and induction of systemic resistance in tomato against early and late blight by
797 Bacillus subtilis OTPB1 or Trichoderma harzianum OTPB3. Biological Control *65*, 109–117.
798 https://doi.org/10.1016/j.biocontrol.2012.11.009.

799 53. Lian, L., Xie, L., Zheng, L., and Lin, Q. (2011). Induction of systemic resistance in tobacco
800 against Tobacco mosaic virus by Bacillus spp. Biocontrol Sci Technol *21*, 281–292.
801 https://doi.org/10.1080/09583157.2010.543667.

802 54. Guo, Q., Li, Y., Lou, Y., Shi, M., Jiang, Y., Zhou, J., Sun, Y., Xue, Q., and Lai, H. (2019). Bacillus
803 amyloliquefaciens Ba13 induces plant systemic resistance and improves rhizosphere
804 microecology against tomato yellow leaf curl virus disease. Applied Soil Ecology *137*, 154–166.
805 https://doi.org/10.1016/j.apsoil.2019.01.015.

806 55. Srivastava, S., Bist, V., Srivastava, S., Singh, P.C., Trivedi, P.K., Asif, M.H., Chauhan, P.S., and
807 Nautiyal, C.S. (2016). Unraveling aspects of Bacillus amyloliquefaciens mediated enhanced

808 production of rice under biotic stress of Rhizoctonia solani. Front Plant Sci *7*.
809 https://doi.org/10.3389/fpls.2016.00587.

810 56. Yasmin, S., Zaka, A., Imran, A., Zahid, M.A., Yousaf, S., Rasul, G., Arif, M., and Mirza, M.S.
811 (2016). Plant growth promotion and suppression of bacterial leaf blight in rice by inoculated
812 bacteria. PLoS One *11*. https://doi.org/10.1371/journal.pone.0160688.

813 57. Mehmood, S., Muneer, M.A., Tahir, M., Javed, M.T., Mahmood, T., Afridi, M.S., Pakar, N.P.,
814 Abbasi, H.A., Munis, M.F.H., and Chaudhary, H.J. (2021). Deciphering distinct biological control
815 and growth promoting potential of multi-stress tolerant Bacillus subtilis PM32 for potato stem
816 canker. Physiology and Molecular Biology of Plants *27*, 2101–2114.
817 https://doi.org/10.1007/s12298-021-01067-2.

818 58. Zamioudis, C., Korteland, J., Van Pelt, J.A., Van Hamersveld, M., Dombrowski, N., Bai, Y.,
819 Hanson, J., Van Verk, M.C., Ling, H.Q., Schulze-Lefert, P., et al. (2015). Rhizobacterial volatiles
820 and photosynthesis-related signals coordinate MYB72 expression in Arabidopsis roots during
821 onset of induced systemic resistance and iron-deficiency responses. Plant Journal *84*, 309–
822 322. https://doi.org/10.1111/tpj.12995.

823 59. Wu, L., Huang, Z., Li, X., Ma, L., Gu, Q., Wu, H., Liu, J., Borriss, R., Wu, Z., and Gao, X. (2018).
824 Stomatal closure and SA-, JA/ET-signaling pathways are essential for Bacillus
825 amyloliquefaciens FZB42 to restrict leaf disease caused by Phytophthora nicotianae in
826 Nicotiana benthamiana. Front Microbiol *9*. https://doi.org/10.3389/fmicb.2018.00847.

827 60. Cawoy, H., Mariutto, M., Henry, G., Fisher, C., Vasilyeva, N., Thonart, P., Dommes, J., and
828 Ongena, M. (2014). Plant defense stimulation by natural isolates of Bacillus depends on
829 efficient surfactin production. Molecular Plant-Microbe Interactions *27*, 87–100.
830 https://doi.org/10.1094/MPMI-09-13-0262-R.

831 61. Zebelo, S., Song, Y., Kloepper, J.W., and Fadamiro, H. (2016). Rhizobacteria activates (+)-δ-
832 cadinene synthase genes and induces systemic resistance in cotton against beet armyworm
833 (Spodoptera exigua). Plant Cell Environ *39*, 935–943. https://doi.org/10.1111/pce.12704.

834 62. Ravanbakhsh, M., Sasidharan, R., Voesenek, L.A.C.J., Kowalchuk, G.A., and Jousset, A. (2018).
835 Microbial modulation of plant ethylene signaling: ecological and evolutionary consequences.
836 Microbiome *6*. https://doi.org/10.1186/s40168-018-0436-1.

837 63. Berrabah, F., Balliau, T., Aït-Salem, E.H., George, J., Zivy, M., Ratet, P., and Gourion, B. (2018).
838 Control of the ethylene signaling pathway prevents plant defenses during intracellular
839 accommodation of the rhizobia. New Phytologist *219*, 310–323.
840 https://doi.org/10.1111/nph.15142.

841 64. Carlew, S.S., Brenya, E., Ferdous, M., Banerjee, I., Donnelly, L., Heinze, E., King, J., Sexton, B.,
842 Lacey, R.F., Bakshi, A., et al. (2025). Ethylene signals through an ethylene receptor to
843 modulate biofilm formation and root colonization in a beneficial plant-associated bacterium.
844 PLoS Genet *21*. https://doi.org/10.1371/journal.pgen.1011587.

845 65. Das, D., Varshney, K., Ogawa, S., Torabi, S., Hüttl, R., Nelson, D.C., and Gutjahr, C. (2025).
846 Ethylene promotes SMAX1 accumulation to inhibit arbuscular mycorrhiza symbiosis. Nature
847 Communications *16*. https://doi.org/10.1038/s41467-025-57222-w.

848 66. Knoester, M., Pieterse, C.M.J., Bol, J.F., and Van Loon, L.C. (1999). Systemic Resistance in
849 Arabidopsis Induced by Rhizobacteria Requires Ethylene-Dependent Signaling at the Site of

850 Application. Molecular Plant-Microbe Interactions *12*, 720–727.
851 https://doi.org/10.1094/MPMI.1999.12.8.720.

852 67. Lidoy, J., Rivero, J., Ramšak, Ž., Petek, M., Križnik, M., Flors, V., Lopez-Raez, J.A., Martinez-
853 Medina, A., Gruden, K., and Pozo, M.J. (2025). Ethylene signaling is essential for mycorrhiza-
854 induced resistance against chewing herbivores in tomato. J Exp Bot.
855 https://doi.org/10.1093/jxb/eraf053.

856 68. Huang, P.Y., Catinot, J., and Zimmerli, L. (2016). Ethylene response factors in Arabidopsis
857 immunity. J Exp Bot *67*, 1231–1241. https://doi.org/10.1093/jxb/erv518.

858 69. Chowdhury, S.P., Uhl, J., Grosch, R., Alquéres, S., Pittroff, S., Dietel, K., Schmitt-Kopplin, P.,
859 Borriss, R., and Hartmann, A. (2015). Cyclic lipopeptides of Bacillus amyloliquefaciens subsp.
860 plantarum colonizing the lettuce rhizosphere enhance plant defense responses toward the
861 bottom rot pathogen Rhizoctonia solani. Molecular Plant-Microbe Interactions *28*, 984–995.
862 https://doi.org/10.1094/MPMI-03-15-0066-R.

863 70. Zhou, J., Tang, X., and Martin, G.B. (1997). The Pto kinase conferring resistance to tomato
864 bacterial speck disease interacts with proteins that bind a cis-element of pathogenesis-related
865 genes. EMBO J *16*, 3207–3218. https://doi.org/10.1093/emboj/16.11.3207.

866 71. He, P., Warren, R.F., Zhao, T., Shan, L., Zhu, L., Tang, X., and Zhou, J.-M. (2001).
867 Overexpression of Pti5 in Tomato Potentiates Pathogen-Induced Defense Gene Expression
868 and Enhances Disease Resistance to Pseudomonas syringae pv. tomato. Molecular Plant-
869 Microbe Interactions *14*, 1453–1457. https://doi.org/10.1094/MPMI.2001.14.12.1453.

870 72. Lukan, T., Veillet, F., Križnik, M., Coll, A., Mahkovec Povalej, T., Pogačar, K., Stare, K., Chauvin,
871 L., Chauvin, J.E., and Gruden, K. (2022). CRISPR/Cas9-mediated fine-tuning of miRNA
872 expression in tetraploid potato. Hortic Res *9*. https://doi.org/10.1093/hr/uhac147.

873 73. Lukan, T., Županič, A., Mahkovec Povalej, T., Brunkard, J.O., Kmetič, M., Juteršek, M., Baebler,
874 Š., and Gruden, K. (2023). Chloroplast redox state changes mark cell-to-cell signaling in the
875 hypersensitive response. New Phytologist *237*, 548–562. https://doi.org/10.1111/nph.18425.

876 74. Lukan, T., Machens, F., Coll, A., Baebler, Š., Messerschmidt, K., and Gruden, K. (2018). Plant X-
877 tender: An extension of the AssemblX system for the assembly and expression of multigene
878 constructs in plants. PLoS One *13*. https://doi.org/10.1371/journal.pone.0190526.

879 75. Stefanic, P., and Mandic-Mulec, I. (2009). Social interactions and distribution of Bacillus
880 subtilis pherotypes at microscale. J Bacteriol *191*, 1756–1764.
881 https://doi.org/10.1128/JB.01290-08.

882 76. Tortosa, P., Logsdon, L., Kraigher, B., Itoh, Y., Mandic-Mulec, I., and Dubnau, D. (2001).
883 Specificity and genetic polymorphism of the Bacillus competence quorum-sensing system. J
884 Bacteriol *183*, 451–460. https://doi.org/10.1128/JB.183.2.451-460.2001.

885 77. Pramanik, R.S., Chandwani, S., and Amaresan, N. (2023). Screening of Endophytes for Plant
886 Growth-Promoting Metabolites A. Sankaranarayanan, N. Amaresan, and M. K. Dwivedi, eds.
887 (Springer Protocols Handbooks). https://doi.org/10.1007/978-1-0716-2827-0_19.

888 78. Chabot, S., Bécard, G., and Piché, Y. (1992). Life Cycle of Glomus Intraradix in Root Organ
889 Culture. Mycologia *84*, 315–321. https://doi.org/10.1080/00275514.1992.12026144.

890 79. García, J.M., Pozo, M.J., and López-Ráez, J.A. (2020). Histochemical and Molecular
891 Quantification of Arbuscular Mycorrhiza Symbiosis M. Rodríguez-Concepción and R. Welsch,
892 eds. (Humana, New York, NY) https://doi.org/10.1007/978-1-4939-9952-1_22.

893 80. GIOVANNETTI, M., and MOSSE, B. (1980). An evaluation of techniques for measuring vesicular
894 arbuscular mycorrhizal infection in roots. New Phytologist *84*, 489–500.
895 https://doi.org/10.1111/j.1469-8137.1980.tb04556.x.

896 81. Petek, M., Rotter, A., Kogovšek, P., Baebler, Š., Mithöfer, A., and Gruden, K. (2014). Potato
897 virus Y infection hinders potato defence response and renders plants more vulnerable to
898 Colorado potato beetle attack. Mol Ecol *23*, 5378–5391. https://doi.org/10.1111/mec.12932.

899 82. Baebler, Š., Svalina, M., Petek, M., Stare, K., Rotter, A., Pompe-Novak, M., and Gruden, K.
900 (2017). quantGenius: Implementation of a decision support system for qPCR-based gene
901 quantification. BMC Bioinformatics *18*. https://doi.org/10.1186/s12859-017-1688-7.

902 83. Livak, K.J., and Schmittgen, T.D. (2001). Analysis of relative gene expression data using real-
903 time quantitative PCR and the 2-ΔΔCT method. Methods *25*, 402–408.
904 https://doi.org/10.1006/meth.2001.1262.

905 84. Morcillo, R.J.L., Navarrete, M.I.T., Bote, J.A.O., Monguio, S.P., and García-Garrido, J.M. (2016).
906 Suppression of allene oxide synthase 3 in potato increases degree of arbuscular mycorrhizal
907 fungal colonization. J Plant Physiol *190*, 15–25. https://doi.org/10.1016/j.jplph.2015.11.003.

908 85. R Core Team (2023). R: A Language and Environment for Statistical Computing. R Foundation
909 for Statistical Computing, Vienna. https://www.R-project.org/.

910 86. R Core Team (2021). R: A Language and Environment for Statistical Computing. R Foundation
911 for Statistical Computing, Vienna. https://www.R-project.org/.

912 87. Wickham, H. (2009). ggplot2 1st ed. (Springer New York). https://doi.org/10.1007/978-0-387-
913 98141-3.

914 88. Kassambara, A. (2019). rstatix: Pipe-Friendly Framework for Basic Statistical Tests. Preprint,
915 https://doi.org/10.32614/CRAN.package.rstatix.

916 89. Kassambara, A. (2016). ggpubr: "ggplot2" Based Publication Ready Plots. Preprint,
917 https://doi.org/10.32614/CRAN.package.ggpubr.

918 90. Krueger, F. (2021). Trimgalore . GitHub repository.
919 https://github.com/FelixKrueger/TrimGalore.

920 91. Andrews, S. (2010). FastQC: A Quality Control Tool for High Throughput Sequence Data
921 [Online]. Babraham Bioinformatics.
922 http://www.bioinformatics.babraham.ac.uk/projects/fastqc/.

923 92. Kim, D., Song, L., Breitwieser, F.P., and Salzberg, S.L. (2016). Centrifuge: rapid and sensitive
924 classification of metagenomic sequences. Genome Res *26*, 1721–1729.
925 https://doi.org/10.1101/gr.210641.116.

926 93. Dobin, A., Davis, C.A., Schlesinger, F., Drenkow, J., Zaleski, C., Jha, S., Batut, P., Chaisson, M.,
927 and Gingeras, T.R. (2013). STAR: ultrafast universal RNA-seq aligner. Bioinformatics *29*, 15–21.
928 https://doi.org/10.1093/bioinformatics/bts635.

929 94. Petek, M., Zagorščak, M., Ramšak, Ž., Sanders, S., Tomaž, Š., Tseng, E., Zouine, M., Coll, A., and
930 Gruden, K. (2020). Cultivar-specific transcriptome and pan-transcriptome reconstruction of
931 tetraploid potato. Sci Data *7*. https://doi.org/10.1038/s41597-020-00581-4.

932 95. Subramanian, A., Tamayo, P., Mootha, V.K., Mukherjee, S., Ebert, B.L., Gillette, M.A.,
933 Paulovich, A., Pomeroy, S.L., Golub, T.R., Lander, E.S., et al. (2005). Gene set enrichment
934 analysis: A knowledge-based approach for interpreting genome-wide expression profiles. Proc
935 Natl Acad Sci U S A *102*, 15545–15550. https://doi.org/10.1073/pnas.0506580102.

936 96. Rotter, A., Usadel, B., Baebler, S., Stitt, M., and Gruden, K. (2007). Adaptation of the MapMan
937 ontology to biotic stress responses: application in solanaceous species. Plant Methods *3*.
938 https://doi.org/10.1186/1746-4811-3-10.

939 97. Ramšak, Ž., Petek, M., and Baebler, Š. (2021). RNA Sequencing Analyses for Deciphering
940 Potato Molecular Responses. In Solanum tuberosum, D. Dobnik, K. Gruden, Ž. Ramšak, and A.
941 Coll, eds. (Humana, New York, NY), pp. 57–94. https://doi.org/10.1007/978-1-0716-1609-3_3.

942 98. Garrido Rodríguez-Córdoba, M. (2023). biokit: Toolkit for the automatic analysis of omics
943 data. github. https://github.com/martingarridorc/biokit.

944 99. Ritchie, M.E., Phipson, B., Wu, D., Hu, Y., Law, C.W., Shi, W., and Smyth, G.K. (2015). Limma
945 powers differential expression analyses for RNA-sequencing and microarray studies. Nucleic
946 Acids Res *43*, e47. https://doi.org/10.1093/nar/gkv007.

947 100. Zagorščak, M., Blejec, A., Ramšak, Ž., Petek, M., Stare, T., and Gruden, K. (2018). DiNAR:
948 Revealing hidden patterns of plant signalling dynamics using Differential Network Analysis in
949 R. Plant Methods *14*. https://doi.org/10.1186/s13007-018-0345-0.

950 101. Camacho, C., Coulouris, G., Avagyan, V., Ma, N., Papadopoulos, J., Bealer, K., and Madden, T.L.
951 (2009). BLAST+: Architecture and applications. BMC Bioinformatics *10*.
952 https://doi.org/10.1186/1471-2105-10-421.

953

954 **Supplemental information**

955 Figure S1: Biofilm on potato roots after incubation in *B. subtilis* culture, imaged at different time
956 points.

957 Figure S2: Expression profiles of selected genes.

958 Figure S3: Number of genes, regulated by *B. subtilis* in plants incubated in *B. subtilis* culture of high
959 density (107 CFU/m^{L}).

960 Figure S4: Observation of *B. subtilis* cells in potato tissue after internalization.

961 Figure S5: B. subtilis cells as observed in liquid culture (A) and potato leaf homogenate (B).

962 Figure S6: Biofilm formation on potato roots inoculated with *B. subtilis* mutants that have attenuated
963 surfactin production.

964 Figure S7: *B. subtilis*-produced secondary metabolites in the medium do not contribute significantly
965 to the PTI5 and 13-LOX upregulation.

966 Figure S8: Regulated central signaling modules in potato roots in isogenic and non-kin interactions.

967 Figure S9: *B. subtilis* root colonization of transgenic potato lines with silenced PTI5 (shPTI5 L2 and L6)
968 and non-transgenic (NT) potato plant.

969 Figure S10: Mycorrhizal colonization of potato roots in non-transgenic potato plant (NT) and PTI5
970 silenced genotype line 2 (shPTI5).

971 Table S1: Standardised qPCR gene expression data.

972 Table S2: Results of gene set enrichment analysis.

973 Table S3: Differential gene expression table for comparisons between plants inoculated with *B.*
974 *subtilis* and non-inoculated plants.

975 Table S4: The amount of biofilm on potato roots.

976 Table S5: Relative gene expression in potato inoculated with *B. subtilis* mutants that have attenuated
977 surfactin production.

978 Table S6: Expression of selected potato genes induced by conditioned medium in which *B. subtilis*
979 was growing.

980 Table S7: Plant stress signaling (PSS) prior knowledge network node information with corresponding
981 RNA-seq differential expression.

982 Table S8: The amount of biofilm formation on potato roots for non-transgenic (NT) and shPTI5 plants.

983 Table S9: *B. subtilis* abundance in shPTI5 L6 and non-transgenic (NT) potato plants determined by
984 qPCR.

985 Table S10: *B. subtilis* abundance in shPTI5 L2 and non-transgenic (NT) potato plants determined by
986 qPCR.

987 Table S11: Abundance of *B. subtilis* PS-216 and QS impaired strain PS-216 *srfA* in Rywal non-
988 transgenic (NT) potato plants, determined by qPCR.

989 Table S12: The production of indole acetic acid (IAA) was assessed following the protocol of Pramanik
990 et al.[77]

991 Table S13: Selected genes and corresponding primers and probes sequences for expression analyses
992 with quantitative PCR.

993 Table S14: Sample information for RNA-seq experiments.

994